ELSEVIER

Palaeogeography, Palaeoclimatology, Palaeoecology 131 (1997) 433–463

PALAEO

Late Quaternary palaeoceanography near Tasmania, southern Australia

V. Passlow [a,1], Wang Pinxian [b], A.R. Chivas [c]

[a] *Australian Marine Quaternary Program, Department of Geology, The Australian National University, Canberra 0200, Australia*

[b] *Department of Marine Geology, Tongji University, Shanghai 200092, P.R. China*

[c] *School of Geosciences, University of, Wollongong, 2522, Australia*

Received 8 May 1995; accepted 27 May 1996

Abstract

This study of the palaeoceanographic record south of Australia is based on two cores taken from lower Circumpolar Deep Water depths: core E27-30, located south of Tasmania in water depth of 3552 m, to the north of the present location of the Subtropical Convergence, and core E55-6 from the continental margin off Victoria at 2346 m depth, in a region of very low surface productivity.

A preliminary examination of planktonic foraminiferal faunas in core E27-30, located south of Tasmania, provides a record of movement of the Subtropical Convergence through the late Quaternary that is consistent with records elsewhere in the Southeast Indian Ocean. The Convergence has been located equatorward of its present position through much of the late Quaternary, with poleward excursions in the Holocene and at oxygen-isotope stage 5e.

Benthic foraminiferal faunas contrast strongly in the two cores, despite their location at similar depths within the same water mass. Core E55-6 is largely dominated by deep infaunal taxa, while core E27-30 has a high proportion throughout of epifaunal taxa. The benthic foraminiferal fauna in core E27-30 is dominated by *Epistominella exigua*, known to feed directly on phytoplankton detritus in the modern deep-sea. Abundances of that species coincide with the presence of the Subtropical Convergence at or near the site, indicating that surface phytoplankton production has had a major influence on benthic productivity.

Dissolution records in the two cores also differ markedly. Core E55-6 records a strong dissolution event in oxygen-isotope stage 4. The cause of the event is not clear, although it appears to be associated with increased productivity levels. This pronounced dissolution event is not evident in core E27-30, suggesting either the event is localised or that the record in core E27-30 has been overprinted by the Convergence.

The extent to which the records in the two cores vary emphasises the influence of frontal structures on core records in this region and the need to take this into account when investigating Southern Ocean history. © 1997 Elsevier Science B.V.

Keywords: ocean circulation; Ostracoda; phytoplankton; productivity

[1]Present address: Australian Geological Survey Organisation, GPO Box 378, Canberra, ACT 2601, Australia.

PII S0031-0182(97)00015-1

1. Introduction

The Subtropical Convergence (STC) is an important component of the southeast Indian/Southern Ocean frontal structure, which in the Australasian sector includes the Antarctic Polar Front and the Subantarctic Front. The Subtropical Convergence, like other frontal structures, is formed in response to high-latitude wind fields and can be recognised by distinctive surface-water temperature, salinity and productivity characteristics. The front is also recognised as the boundary between the southeast Indian Ocean to the north and the Southern Ocean to the south.

Changes in the palaeolatitude of the STC through the Quaternary have been well documented in the southern Indian and southeastern Indian Oceans west of Australia (Hays et al., 1976; Williams, 1976; Prell et al., 1979; Prell et al., 1980; Morley, 1989; Howard and Prell, 1992). These studies place the STC equatorward of its present position through much of the Quaternary. Poleward movement of the front has been recorded only four times during the past 500,000 yr (Howard and Prell, 1992): during the Holocene, at oxygen-isotope stage 5e (≈128–118 ka), stage 9 (≈340–330 ka) and stage 11 (≈425–390 ka), with maximum poleward extents during stages 9 and 11. Francois et al. (1993), in a study of sediment rain rate from a core located south of the Subantarctic Front, also recorded southward movement of the STC during the early Holocene (at approximately 7.5–10 ka). Other studies generally agree in the sense and magnitude of these movements, although Prell et al. (1979) located the STC north of 41° S during stages 1 and 5, and Morley's radiolarian-based study (1989) did not record a poleward shift at stage 9.

Sea surface palaeotemperature (SST) estimates in the region of the STC, based on different biogenic parameters, generally show good agreement. These include the radiolarian-based studies of Morley (1989) and Morley et al. (1988), the planktonic foraminiferal estimates of Labracherie et al. (1989) and Howard and Prell (1992) and diatom-based estimates of Pichon et al. (1992). The 10°C isotherm, which marks the present winter polar edge of the STC, has been equatorward of 42° S through the Quaternary, except during the four poleward excursions. The maximum southward extent of approximately 45° S occurred during stages 9 and 11 (Howard and Prell, 1992).

The modern STC zone is characterised by high seasonal phytoplankton production, in contrast with subantarctic waters (Plancke, 1977; Jacques and Minas, 1981; Lutjeharms et al., 1985; Francois et al., 1994) and subtropical waters north of the STC in the Australian region (Highley, 1968). As a result of high phytoplankton production, the STC region is likely to have enhanced flux to the seafloor (Francois et al., 1993). Evidence of this has been found in modern sediments beneath the STC and Southern Ocean frontal structures in the South Atlantic (Mackensen et al., 1993). Results of the latter study suggest that increased productivity associated with frontal structures may partially account for Southern Ocean $\delta^{13}C$ values. Recognition of the impact of frontal structures is therefore significant in the interpretation of Southern Ocean chemistry and its role in global climate.

This study documents the palaeoceanographic record in two cores offshore southeastern Australia (Fig. 1), a region where the palaeoceanography of the STC has not been well documented. Core E55-6 is taken from a water depth of 2346 m on the continental margin of mainland Australia. Core E27-30, from a depth of 3552 m, is located south of Tasmania and to the north of the Subtropical Convergence. Variations in planktonic

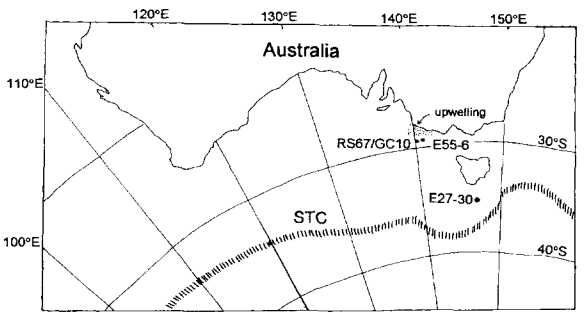

Fig. 1. Locations of the cores examined in this study. The approximate position of the Subtropical Convergence (STC) is indicated.

foraminiferal assemblages are used to provide a preliminary record of movement of the STC. Comparisons between the palaeoceanographic records in the cores are also made to evaluate the extent to which the STC has affected planktonic and benthic records.

2. The modern setting

2.1. Oceanography of the study area

Regional water mass profiles from the study area, showing intermediate and deep-water mass boundaries are provided in Fig. 2. Water-mass data are taken from two regions: adjacent to the southeastern Australian mainland (co-ordinates 36°S–42°S, 134°E–144°E) and south of Tasmania (co-ordinates 44°S–50°S, 144°E–149°E). The characteristics of intermediate and deep-water masses in these regions are summarised in Table 1. Unpublished water mass data were provided by the Commonwealth Scientific and Industrial Research Organisation (CSIRO) and the Australian Oceanographic Data Centre. Published cruise data from the region (CSIRO Division of Fisheries and Oceanography, 1962, 1966, 1967a,b) were also incorporated.

Surface waters adjacent to the southern margin are largely subtropical in origin and are characterised by low productivity levels (Highley, 1968; see Fig. 2D). Weak, wind-driven upwelling occurs

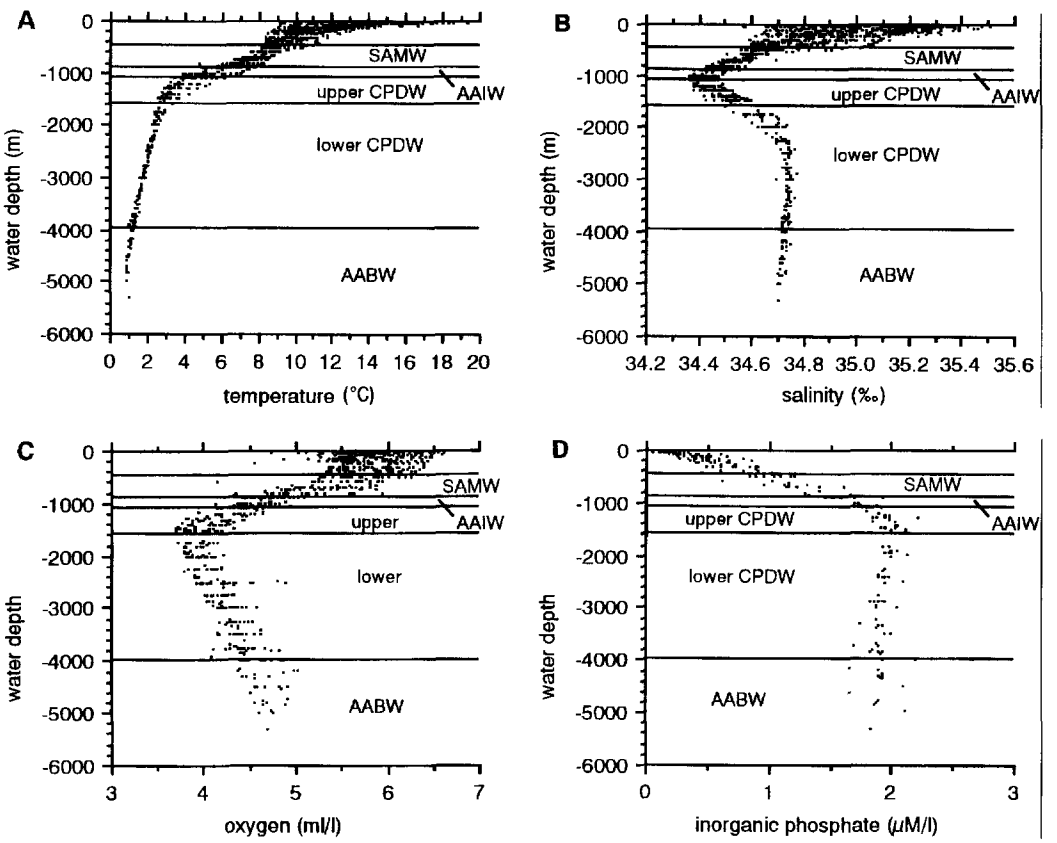

Fig. 2. Water mass profiles, showing boundaries of Subantarctic Mode Water (*SAMW*), Antarctic Intermediate Water (*AAIW*), upper and lower Circumpolar Deep Water (*CPDW*) and Antarctic Bottom Water (*AABW*). Data are taken from the region adjacent to the southeastern Australian mainland (co-ordinates 36°S–42°S, 134°E–144°E) and south of Tasmania (co-ordinates 44°S–50°S, 144°E–149°E).

Table 1
Characteristics of the intermediate and deep-water masses in the study area (see text for regions included)

Water mass	Depth range (m)	Temperature (°C)	Salinity (‰)	Dissolved oxygen (ml/l)
Subantarctic Mode Water	450–850	10–8	34.5–34.6	5.6–4.5
Antarctic Intermediate Water	850–1100	8–4	34.4	4.5–4
upper Circumpolar Deep Water	1100–1600	4–2.8	34.4–34.6	4.0
lower Circumpolar Deep Water	1600–4000	2.8–1.1	34.72	4.0–4.5
Antarctic Bottom Water	>4000	1.1–0.9	34.70–34.72	4.5–5

during austral summer months on a section of the coastline (Fig. 1). Upwelling events occur unevenly across the shelf, tending to be localised in extent and duration (Rochford, 1977; Schahinger, 1987). Cooler, less saline water is brought up from depths of around 250–300 m. Upwelled waters also show a large increase in nutrient levels (Rochford, 1977) and therefore have implications for the productivity of surface waters.

South of Tasmania, surface waters are influenced by the Subtropical Convergence (STC) and its associated high seasonal phytoplankton production. The STC was originally recognised south of Tasmania, between 42° and 45° S, by Deacon (1937), based on a sharp increase in salinity (34.6–35.1‰) and temperature (11–13.5°C) from south to north. Gordon (1972) also observed the same salinity gradient at a depth of 20 m between 42° and 45° S. However, Edwards and Emery (1982) located the austral summer position of the STC further to the south (45°–46° S) based on an uplift in the isothermal structure.

The STC marks the boundary between warm, saline subtropical surface waters driven by the southeast trade winds and cold, weakly-saline subantarctic surface waters driven by westerly winds (Deacon, 1937; Tchernia, 1980). These converging wind fields cause the position of the STC, which is best considered as a zone, to shift seasonally. Meanders and eddies are also an integral part of the structure of the front (Cresswell et al., 1978; Tchernia, 1980).

Two intermediate waters can be recognised: Antarctic Intermediate Water (AAIW) and Subantarctic Mode Water (SAMW). Recent examination of CFC "ages" of the two water masses in the Indian Ocean (Fine, 1993) suggests separate origins and distribution pathways. SAMW is formed by winter cooling of surface waters north of the Subantarctic Front (McCartney, 1977). The cool surface layer sinks in the summer and is isolated by warmer surface waters, forming a distinct thermostad (a layer characterised by a minimal vertical temperature gradient). In the Australian sector, SAMW is circulated by an anticyclonic gyre which brings it to the continental margin at depths of between 450 and about 850 m (McCartney, 1977; Edwards and Emery, 1982). The thermostad distinguishing SAMW is clearly visible in water mass profiles (Fig. 2A). Underlying AAIW occurs as a salinity minimum layer near the base of the thermocline (Rochford, 1961; Fig. 2; Table 1). AAIW also follows a westward flow south of Australia.

Deep water in the South Australian Basin is defined by Osborne et al. (1983) as Circumpolar Deep Water (CPDW), based on a characteristic salinity minimum core. CPDW is divided into lower CPDW and upper CPDW, separated by the salinity minimum. The different characteristics of upper and lower CPDW (Fig. 2; Table 1) suggest different sources. In the southern Indian Ocean, Park et al. (1993) identified lower CPDW with a salinity maximum and nutrient minimum as being composed of mixed North Atlantic Deep Water (NADW). Upper CPDW is distinguished by an oxygen minimum (Park et al., 1993; Fig. 2C). It appears to be derived from North Indian Deep Water (NIDW) and to enter the South Australian Basin from the west (Rochford, 1965; Park et al., 1993). Both sediment cores examined in this study occur within the depth range of lower CPDW.

Antarctic Bottom Water (AABW) enters the South Australian Basin via the Australian–

Antarctic Discordance. The main direction of AABW flow within the basin is to the west (Kolla et al., 1976; Rodman and Gordon, 1982). AABW in the study area is restricted to depths greater than 4000 m and is characterised by lower salinity and temperature and a higher oxygen content in comparison with CPDW.

2.2. Sediments of the southern Australian margin

The study area forms part of the cool-water carbonate province which extends across the entire southern margin of Australia (Wass et al., 1970; Jones and Davies, 1983). Production of bryozoan-dominated sediments occurs on the outer shelf and upper slope (James et al., 1992; Boreen and James, 1993; Boreen et al., 1993). Sedimentation on the upper and mid-slopes to depths of at least 1500–2300 m is dominated by downslope transport, predominantly mud-flow sediments (Boreen and James, 1993; von der Borch and Hughes-Clarke, 1993; Exon et al., 1994; Passlow, 1994). Transported sediments are largely derived from sediments of the shelf and upper slope, although mid- and lower-slope flows contain an increased proportion of slope fauna. On the lower slopes there is accumulation of hemipelagic sediments, with intermittent mud flow and turbidite activity, primarily during low sea-level stands and subsequent transgressions (Boreen and James, 1993). Mud flow sediments, especially those of the mid- to lower slopes, are typically fine-grained and difficult to distinguish from hemipelagic sediments, except by their composition (Passlow, 1994; Passlow et al., in prep.).

3. Materials and methods

3.1. Core selection and sampling

The locations of cores selected for this study are shown in Fig. 1; details are provided in Table 2. The two cores, *Eltanin* cores E55-6 and E27-30, were selected for minimal sedimentological disturbance, given the high rates of downslope sediment transport in the region. Detailed descriptions of core sediments are included in Passlow (1994).

Table 2
Core location, water depth and sampling

Core	E55-6	E27-30
Lat (°S)	38°51.2'	45°04.0'
Long.(°E)	141°03.8'	147°13.7'
Water depth (m)	2346	3552
Section sampled (cm)	0–390	0–441

Intervals of downslope-transported sediments (mud flows and turbidites) were identified in both cores (Tables 3 and 4). The criteria used to identify these intervals included sedimentary characteristics, such as sandy basal layers, wispy laminae, disturbed laminations, normal grading and the presence of a significant proportion of shallow-water derived taxa, particularly shallow-water ostracods (van Harten, 1986, 1990; Drapala, 1993) and ascidian spicules.

Cores were sampled at a minimum of 10 cm downcore spacing, where possible. Sample size averaged 75 cm^3. Additional closely-spaced samples (5 cm intervals) were taken from the top 3 m of core E55-6 and the top 2 m of core E27-30. All samples were disaggregated in a solution of 5% hydrogen peroxide. Samples were then washed through a 63 μm sieve, oven dried at 25° C and dry sieved into >150 μm and 63–150 μm fractions.

3.2. Micropalaeontological techniques

For planktonic foraminiferal work, subsamples of the >150-μm fraction were taken using a microsplitter. Between 300 and 460 individual planktonic Foraminifera were counted in subsamples (average count 346 individuals) for core E27-30. Foraminiferal abundance data for core E55-6 were based on counts of between 250 and 711 individuals (average count 362 individuals). Species determinations followed the taxonomy of Parker (1962), Bé (1977) and Saito et al. (1981). Fragments of planktonic Foraminifera and the number of benthic Foraminifera were also counted. Benthic Foraminifera were picked from the whole >150-μm fraction or a split of that fraction obtained using a microsplitter (average count 183 individuals).

Table 3
Isotope data and stratigraphic framework for core E55-6

Core depth (cm)	Event	Age (ka)	*G. bulloides* $\delta^{13}C$	*G. bulloides* $\delta^{13}C$ repl.	*G. bulloides* $\delta^{18}O$	*G. bulloides* $\delta^{18}O$ repl.	*Uvigerina* spp. $\delta^{13}C$	*Uvigerina* spp. $\delta^{18}O$
0-33	mud flow							
2		1.0						
5		3.0						
10		5.0						
15		7.0	−0.66		0.35			
20		9.0	25	10.9				
28	2	12.0						
30		12.9						
35		14.9	−0.47	−0.08	2.26	2.45		
40	2.2	17.8	−0.36		2.51		−0.98	4.96
45		18.7	−0.41		2.45			
50		19.6					−1.09	4.96
55		20.5	0.36		2.29			
60		21.4	0.02		2.38		−1.01	4.76
70		23.2	−0.2		2.08		−0.99	4.69
75	3	24.1						
80		26.3	−0.25		1.79		−1.11	4.78
90		30.6	−0.36		1.81		−0.85	4.5
100		35.0	−0.14		1.81		−1.22	4.55
110		39.4	0.17		1.9		−1.09	4.38
120		43.1	−0.18		1.79		−1.16	4.55
130		48.1	−0.16		1.66		−1.01	4.45
140		52.4	−0.56		1.47		−0.88	4.46
150		56.8	−0.69		1.65		−0.97	4.45
155	4	59.0					−1.31	4.63
160		60.7	−0.08		2.15		−1.52	4.65
165		62.4					−1.28	4.63
170		64.2	0.03		2.3		−1.17	4.62
180		67.6					−1.25	4.41
190		71.1	0.28		2.46			
195		72.9	0.36		2.3			
	5	73.9						
200		74.7	−0.21		1.5			
205		76.8	−0.33		1.34		−1.41	3.98
210		78.8	−0.34		1.36		−1.2	4.12
220		82.9	0.47		2.08		−1.36	4.36
230		87.0	−0.25		1.31			
235		89.1					−1.28	3.95
240		91.1	−0.71		0.88		−1.27	3.94
245		93.1					−1.26	3.94
250		95.2	0.32		1.67			
255		97.2					−1.57	3.95
260		99.3	−0.09	−0.3	0.96	1.17		
270		103.4	0.17		1.39			
275		105.4					−1.15	4.03
280		107.5	−0.45		0.92		−1.07	4.06
290		111.5	0.46		0.89			
295		113.6					−1.09	3.86
300		115.6	−0.57		0.74		−1.07	3.71
310		119.7	−0.73		0.63		−1.08	3.79

Table 3 (*continued*)

Core depth (cm)	Event	Age (ka)	*G. bulloides* $\delta^{13}C$	*G. bulloides* $\delta^{13}C$ repl.	*G. bulloides* $\delta^{18}O$	*G. bulloides* $\delta^{18}O$ repl.	*Uvigerina* spp. $\delta^{13}C$	*Uvigerina* spp. $\delta^{18}O$
320	5.5	123.8	−1.08		0.52		−1.11	3.67
330		126.4	−0.92		1		−1.17	3.9
340		129.1	−0.63		1.29		−0.88	3.88
345	6	129.8						
344–350	mud flow							
350			−0.15		1.3		−1.16	4.15
360		132.7	−0.02		1.47			
370		135.3	−0.19		1.24		−1.22	4.03
380		137.0	−0.22		1.3		−1.03	4.01
390		140.6	−0.57		1.01		−1.27	4.03

3.3. Age determinations and stable isotopes

Three AMS ^{14}C dates (Table 5) were obtained using the planktonic foraminifer *Globorotalia inflata*. Approximately 200–250 tests were picked per sample from the >150-μm fraction to provide a minimum weight of 2 mg. Specimens were cleaned in an ultrasonic bath for approximately 5 s, then rinsed twice in ethanol. Initial sample preparation for AMS ^{14}C dating was carried out at the Radiocarbon Dating Research Laboratory of the Research School of Pacific and Asian Studies, ANU. Samples were analysed at the University of Arizona.

Nannofossil smears were prepared from unprocessed core samples using standard preparation techniques (H. Okada, pers. commun., 1992), then mounted on mica and gold sputter-coated for examination under the scanning electron microscope. Nannofossil assemblages were used in age determinations.

Stable-isotope analyses using *Globigerina bulloides* were carried out for cores E55-6 and E27-30 and for core E55-6 using *Uvigerina* spp. The specimen size range for *G. bulloides* was 300–350 μm diameter, sample weights averaged 150 μg. Specimens were agitated in an ultrasonic bath for two periods of approximately 3–5 s each, then rinsed each time in distilled water. Specimens from core E27-30 were too fragile to be cleaned directly in an ultrasonic bath. Specimens from the latter core were soaked for a minimum of 48 h in distilled water, then agitated in an ultrasonic bath with the specimens contained in a heavy glass vessel for additional protection.

Benthic foraminiferal analyses for core E55-6 were carried out using *Uvigerina peregrina* except in one sample, in which *Uvigerina* spp. were used. Specimen preparation techniques for benthic material were similar to those used for planktonic material. In addition, specimens were soaked for two minutes in dilute (0.1%) hydrochloric acid to remove any additional carbonate residue. This procedure was carried out in view of the high carbonate content of sediments from this region (Exon et al., 1989; Passlow, 1994). Oven roasting to remove organic residues was not considered necessary as the samples had been processed initially in hydrogen peroxide. Sample weights for *Uvigerina* averaged 150 μg and samples typically contained 3–5 specimens.

Stable-isotope analyses were carried out at the Environmental Geochemistry Laboratory at the Research School of Earth Sciences, ANU. All samples were analysed on a Finnigan MAT 251 mass spectrometer with an automated acid-on-individual carbonate sample ("Kiel") device. Sample reaction was carried out at a temperature of 90°C and corrections for the temperature effect have been included in sample results. Isotope values were run against the standard NBS-19 and results have been corrected relative to the Peedee belemnite (PDB). See Chivas et al. (1993) for a discussion of techniques and analytical precision. A small number of replicate samples was run for planktonic Foraminifera from each core (Tables 3

Table 4
Isotope data and stratigraphic framework for core E27-30

Core depth (cm)	Event	Age (ka)	*G. bulloides* $\delta^{13}C$	*G. bulloides* $\delta^{13}C$ repl.	*G. bulloides* $\delta^{18}O$	*G. bulloides* $\delta^{18}O$ repl.
1	mud flow		−0.1		2.23	
5.5	^{14}C age		0.44		1.81	
9.5	1.1	2.3	0.22		1.09	
20		5.4	−0.13		1.07	
30		8.4	0.07		0.72	
40	^{14}C age	11.4	−0.49		1.79	
45	2	12.0				
50		14.0	−0.43	−0.12	2.59	2.73
60	2.2	17.8	0.18		2.98	
67–71	mud flow					
80		20.3	0.51		2.82	
90		21.8	0.3		2.6	
98		23.0	0.13		2.55	
105	3	24.1				
110		27.6	−0.02		2.12	
120		34.6	0.01		2.24	
140		48.5	−0.14		2.07	
150		55.5	0.06		2.22	
155	4	59.0				
163–175	turbidite					
180		63.0	0.5	0.05	2.62	2.16
190		66.1	−0.02		2.49	
200		69.2	0.34		1.96	
210		72.3	0.73		2.26	
215	5	73.9				
220		76.2	0.13		1.45	
230		80.8	0.12		1.72	
240		85.5	0.16		1.82	
247–274	turbidite					
280		91.5	0.17		1.81	
290		96.1	−0.12		1.26	
300		100.7	−0.2		1.31	
310		105.3	0.06		1.71	
320		110.0	0.06		2.05	
330		114.6	0.22		2.16	
340		119.2	0.29		1.95	
350	5.5	123.8	−0.42		1.02	
360		127.8	−0.89		1.43	
365	6	129.8				
370		134.4	−0.27	−0.19	2.66	2.73
380		143.5	−0.22		2.92	
390	6.4	152.6	−0.14		2.96	
400		161.7	−0.51		2.7	
410	contamination		−0.36		2.64	
417–441	turbidite					

and 4). Replicate analyses show differences in isotopic values of between ±0.05‰ and ±0.21‰. The larger variations typically occur near intervals of transported sediment, where contamination by older material is most likely to have affected isotopic values.

Table 5
AMS Carbon-14 dating results

Core number	Interval (cm)	Estimated age (yr B.P.)	Actual age (yr B.P.)
E55-6	TC 0–1	<1000	15,505 ± 135
E27-30	4.5–5.5	1500	5835 ± 85
E27-30	39–40	12,000	11,365 ± 105

4. Results

4.1. Core chronologies

Stable isotope data for cores E55-6 and E27-30 are included in Figs. 3 and 4 and Tables 3 and 4 respectively. Also included in Tables 3 and 4 are the stratigraphic control points used in the development of age models for each core. The stratigraphic framework for both cores was developed using $\delta^{18}O$ records of *G. bulloides*. Stable-isotope events recognised are based on Pisias et al. (1984) and the SPECMAP age assignments of Martinson et al. (1987) are used.

The stratigraphic framework for these cores is based primarily on the positions of stage boundaries (Figs. 3 and 4). Additional tie points used are indicated in Tables 3 and 4. Ages between datum points were assigned using linear interpolation. For the purposes of developing age models, turbidites and mud flows are regarded as instantaneous events and are removed from the sediment record; with the exception of sediments from the top of core E55-6, discussed below. The locations of turbidites and mud flows are indicated for each core (Figs. 3 and 4; Tables 3 and 4). Intervals adjacent to sedimentary events showing high levels of sediment contamination were also removed from the record (Tables 3 and 4). The model generally assumes a lack of significant hiatuses. This is based on the nature of the downslope transport, which in general is not strongly erosional (Passlow, 1994) and the similarity of isotopic values from samples above and below contaminated intervals.

Ages obtained from AMS ^{14}C dating are provided in Table 5. Of the two ^{14}C dates available for core E27-30, only that from interval 39–40 cm supports the oxygen-isotope interpretation. The older than expected age of sediments from interval 4.5–5.5 cm is interpreted as due to mixing-in of older material from the overlying mud flow layer (Table 4). Anomalous isotopic enrichment at the top of the core (Fig. 4; Table 4) i.e. within the mud flow interval and immediately below it support this interpretation.

In contrast, oxygen stable isotope values from the top of adjacent trigger core E55-6 are consistent with expected values (Fig. 3). Sedimentological and palaeontological evidence indicates that this portion of the core consists of mud flow sediments. Evidence for this interpretation includes sedimentary structures (sandy basal layer, wispy laminations, sand stringers) and the presence of shallow-water derived fauna (abundant shallow-water ostracods, ascidian spicules, bryozoan fragments). Relative abundances of the main planktonic foraminiferal taxa are consistent with abundances in an adjacent core, RS67/GC10 (Fig. 5), which shows no evidence of contamination. No ^{14}C dates are available from the top of the core, although the top of the adjacent trigger core, TC 55-6, has a ^{14}C age of 15,505 ± 135 yr.

Nannofossil smears were examined from a number of intervals downcore primarily to check for the presence of significant hiatuses in the sediments and to ensure that sediments were late Quaternary in age. Most of the intervals examined contained *E. huxleyi*. Where this species was absent the remaining faunas were typical of the late Quaternary and in strong contrast to the small Gephyrocapsa faunas typical of the zones predating the appearance of *E. huxleyi* (Matsuoka and Okada, 1989). Absence or low numbers of *E. huxleyi* can be attributed to increased dissolution or dilution of the sample by clays (Burns, 1975; S. Shafik, pers. commun., 1992). Both of these effects were observed in smears from glacial intervals. The results indicate that there are no significant hiatuses, such as have been identified in other cores from this region (Exon et al., 1992; Passlow, 1994).

4.2. Planktonic foraminiferal assemblages and surface water masses

A total of fourteen planktonic foraminiferal species are present (full counts are provided in

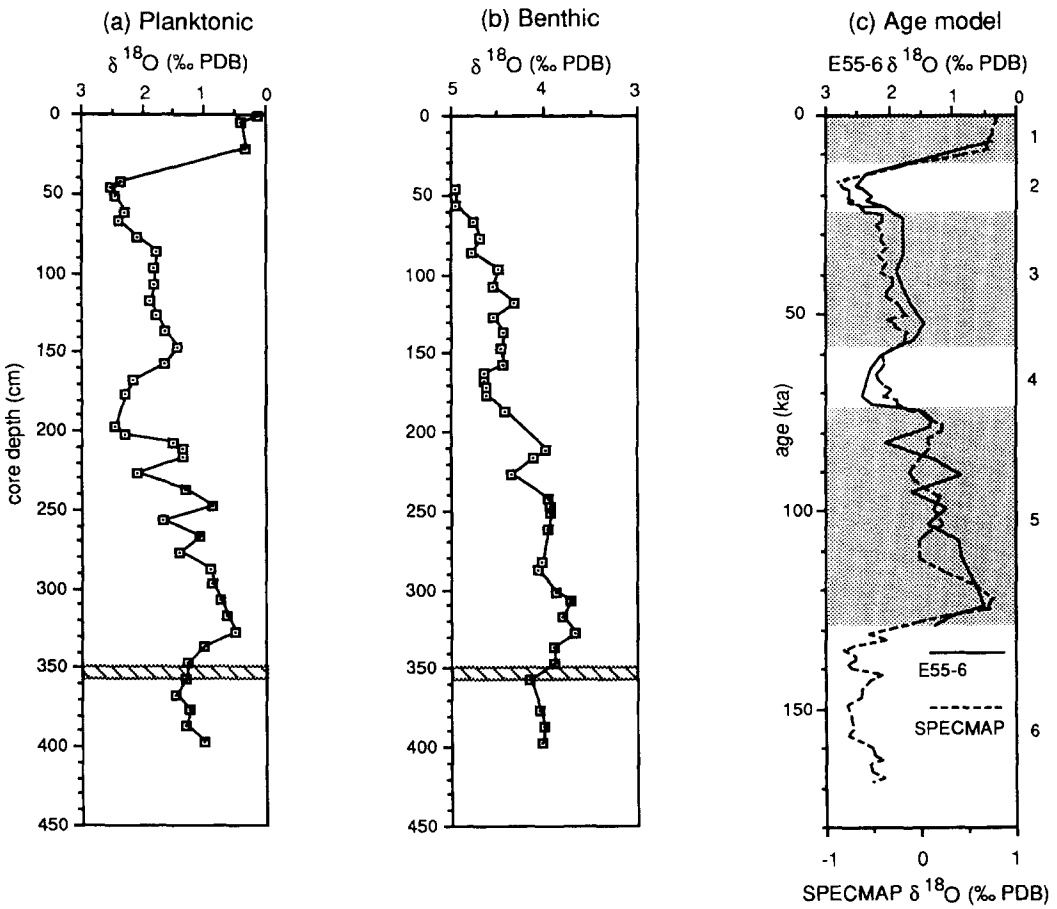

Fig. 3. Oxygen isotope data and age model for core E55-6. (a) Planktonic oxygen-isotope data versus core depth. (b) Benthic oxygen-isotope data versus core depth. (a) and (b) Striped intervals indicate the position of mud flows. (c) Age model, based on planktonic $\delta^{18}O$ data; SPECMAP data from Martinson et al., 1987. Isotopic stages are indicated to the right of the figure, with interglacial periods shaded.

Appendices A and B). Of these, four species account for some 70–90% of the total faunas. These are *Globigerina bulloides*, *Globorotalia inflata*, *Neogloboquadrina pachyderma* and *Globigerina quinqueloba*. Based on modern planktonic foraminiferal biogeography (Bé, 1977), the faunas present in the cores are divided into three groups: a subantarctic group comprising *G. bulloides*, *G. quinqueloba* and sinistral *N. pachyderma*; a transitional group including *G. inflata*, *Neogloboquadrina dutertrei* and dextral *N. pachyderma*; and a subtropical group with *G. truncatulinoides*, *Globigerinoides ruber*, *Globigerina falconensis* and *Globigerinella aequilateralis*. Downcore variations in relative abundance of these groupings are documented for core E55-6 (Fig. 6) and core E27-30 (Fig. 7).

Reconstructions of SST from planktonic Foraminifera have used techniques such as modern analogue or transfer function analysis to derive temperatures. The use of faunal assemblages as a proxy for temperature is limited, as the distribution of planktonic Foraminifera is not controlled directly by temperature. Foraminiferal distribution is influenced by a wide range of ecological factors including also nutrient levels, salinity, species competition and thermal structure of the water column (Bé, 1977; Hemleben et al., 1989). Planktonic

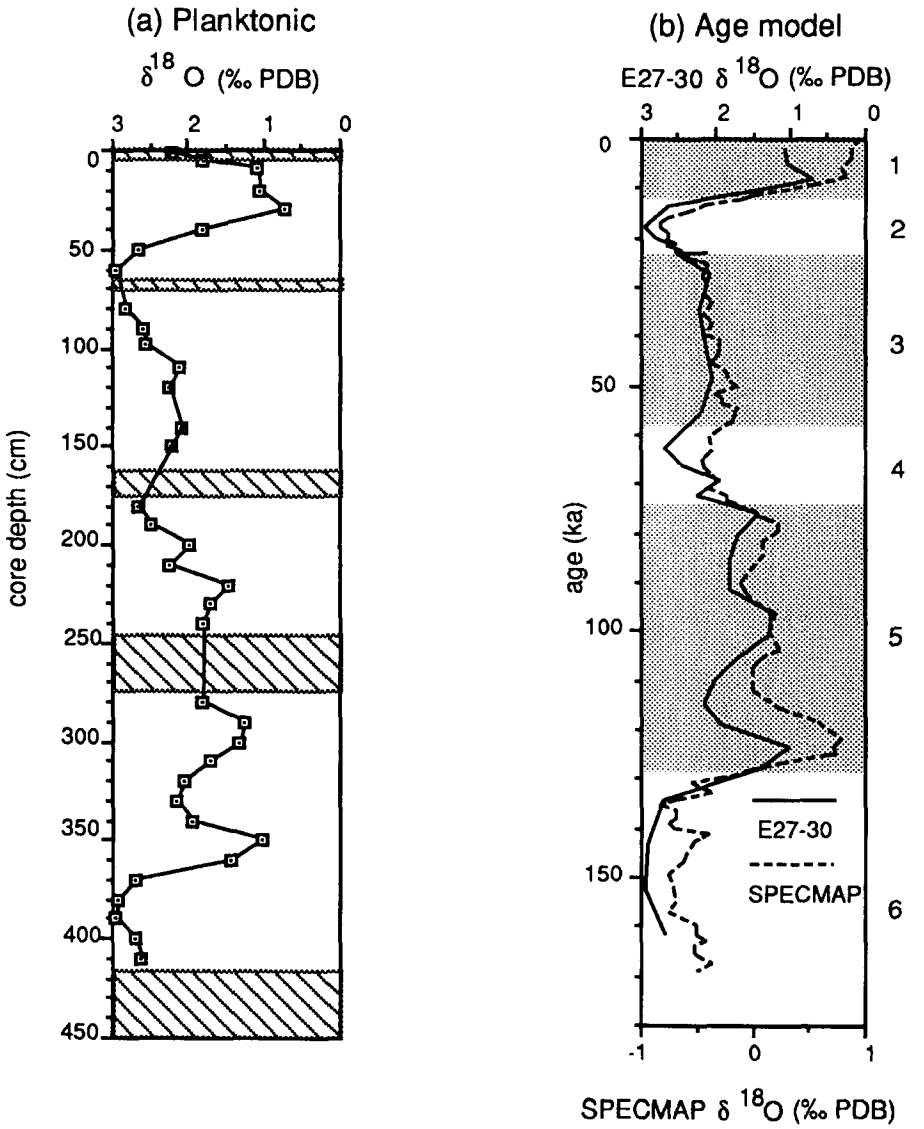

Fig. 4. Oxygen isotope data and age model for core E27-30. (a) Planktonic oxygen-isotope data versus core depth. Striped intervals indicate the position of mud flows and turbidites. (b) Age model, based on planktonic $\delta^{18}O$ data; SPECMAP data from Martinson et al., 1987. Isotopic stages are indicated to the right of the figure, with interglacial periods shaded.

foraminiferal distributions however, have been shown to correspond closely with surface water masses, particularly in the region of the STC (Bé and Tolderlund, 1971; Hutson, 1977; Prell et al., 1979; Howard and Prell, 1992).

Differences between the planktonic foraminiferal faunas in the two cores are consistent with the different surface water masses which affect the two sites. Core E55-6 is influenced largely by waters of subtropical origins and this is reflected by the abundances of subtropical taxa. In comparison, core E27-30, which is located in the transitional region between subtropical and subantarctic waters, to the north of the STC, contains a much

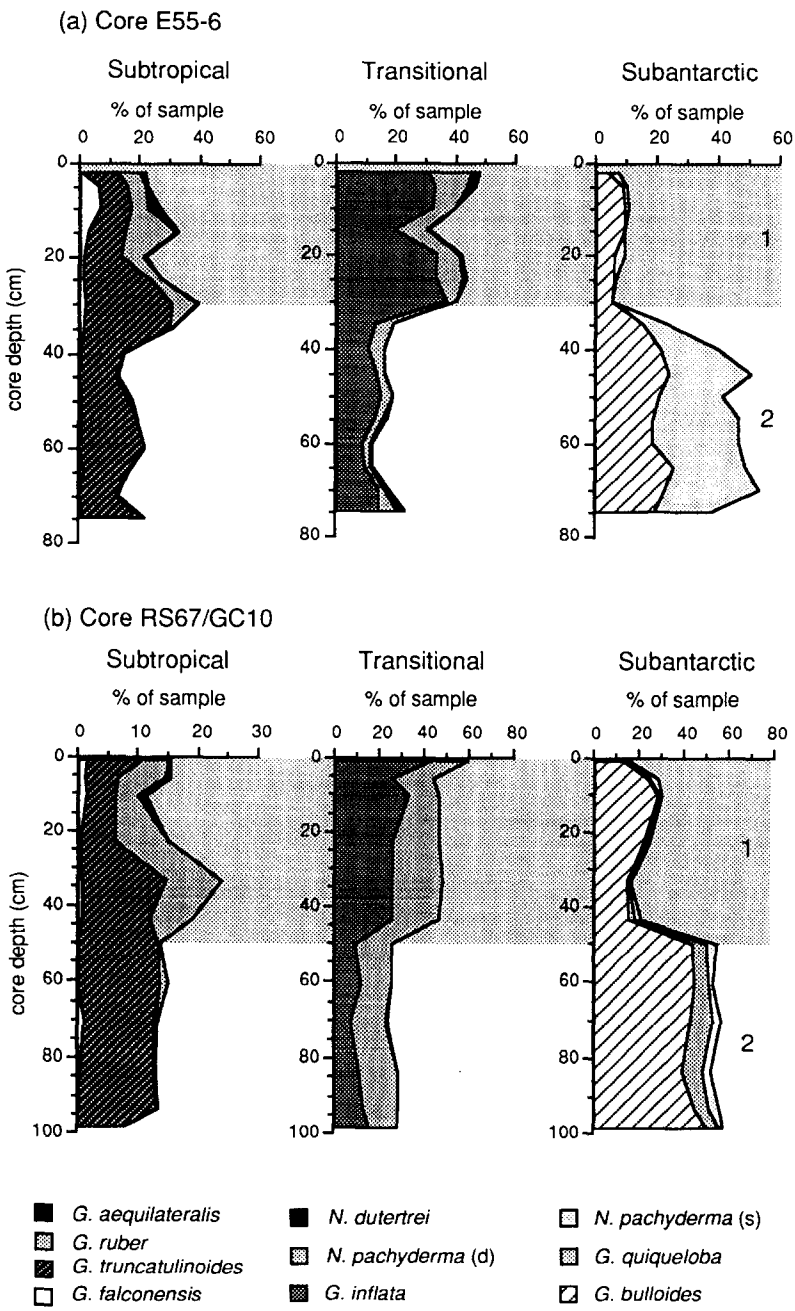

Fig. 5. Comparison of the record of the main planktonic foraminiferal groups through stages 1 and 2 in cores E55-6 and RS67/GC10. Isotopic stages are indicated to the right of each figure, with interglacial periods shaded. Foraminiferal data and isotopic stage boundaries for core RS67/GC10 are taken from Passlow (1994).

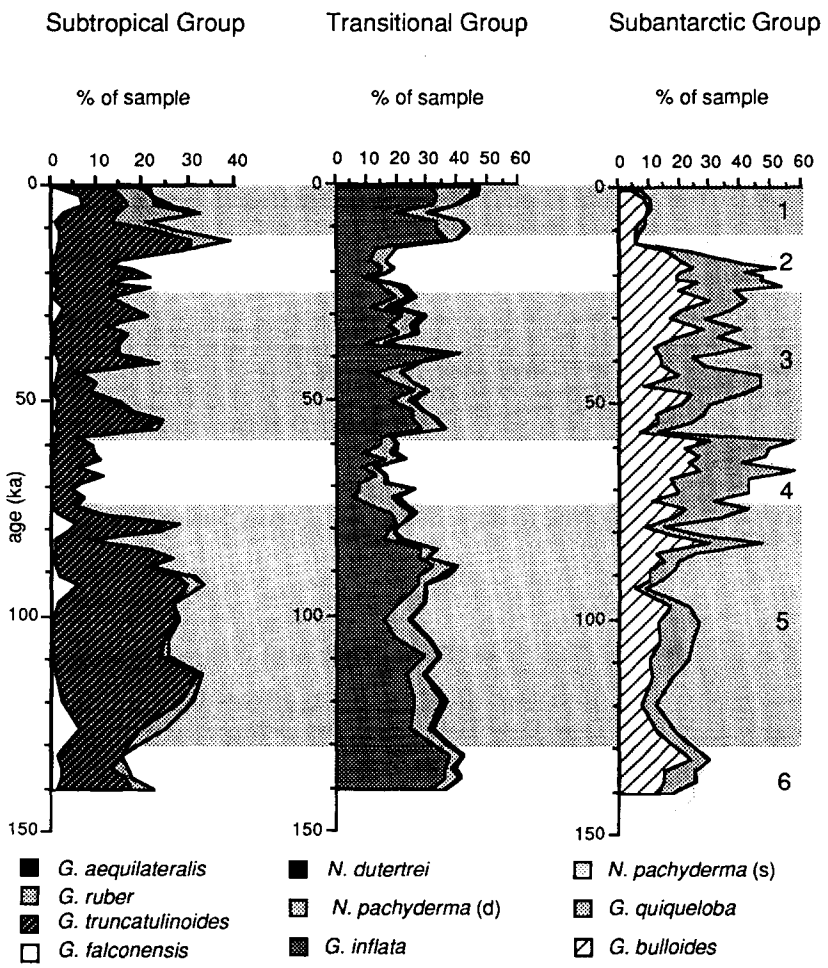

Fig. 6. Relative abundances of the main planktonic Foraminifera within the (a) subtropical, (b) transitional and (c) subantarctic groups in core E55-6. Isotopic stages are indicated to the right of the figure, with interglacial periods shaded.

lower proportion of subtropical taxa. Glacial/interglacial contrasts are present in both cores. In core E55-6 these are shown by all three foraminiferal groups. In core E27-30 they are shown by the relative abundances of the transitional and subantarctic groups. The higher percentage of subtropical taxa in core E55-6 infers warmer SST at that site. Temperature differences are supported by planktonic oxygen-isotope values, which are depleted by some 0.5‰ compared with those of core E27-30 (compare Figs. 3 and 4).

Within core E55-6 there is a marked increase in abundance of *G. bulloides* during glacial stages (Fig. 6). The abundance of *G. quinqueloba* in core E55-6 shows a similar pattern to that of *G. bulloides*. Both of these species have been related to upwelling (Hemleben et al., 1989; Almond et al., 1993). Their increased abundance during glacial stages implies either a distinct decrease in temperature or strengthening of coastal upwelling. The lowering of sea level and subsequent exposure of the shelf may have been responsible for shifting upwelling towards deeper waters and thus over the site of core E55-6. However, it is not possible to separate the effects of cooling from those of increased upwelling on the evidence available here.

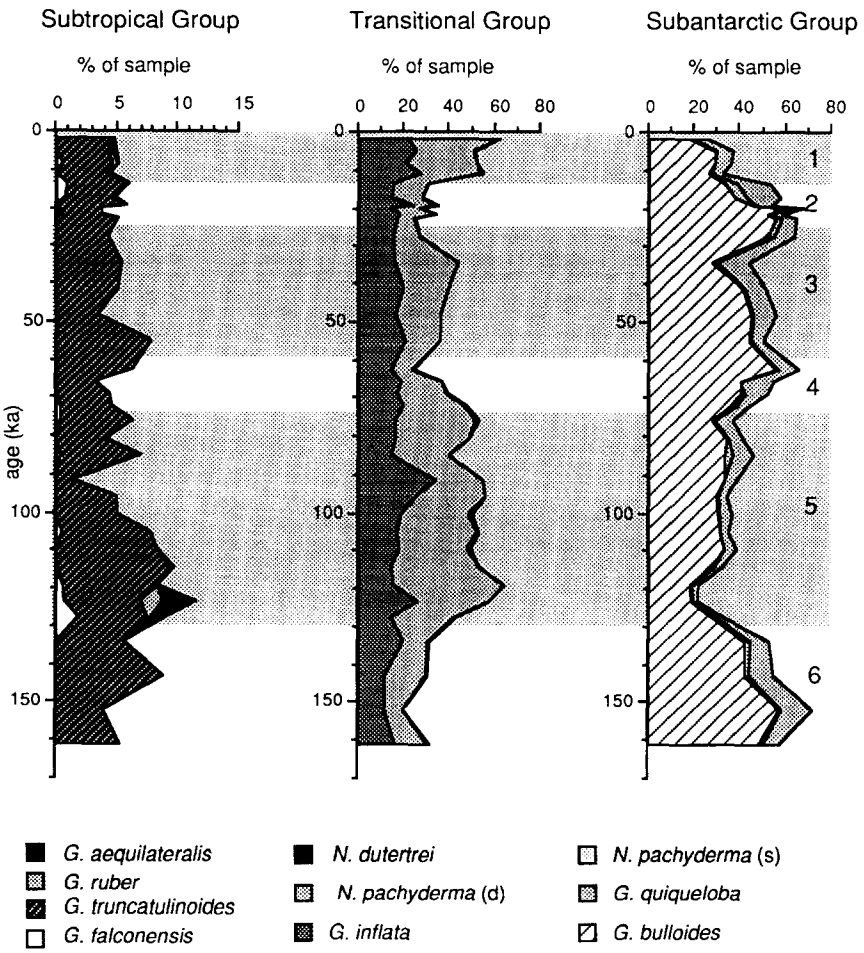

Fig. 7. Relative abundances of the main planktonic Foraminifera within the (a) subtropical, (b) transitional and (c) subantarctic groups in core E27-30. Isotopic stages are indicated to the right of the figure, with interglacial periods shaded.

4.3. Movement of the STC

While faunal changes in core E55-6 follow a glacial/interglacial pattern, the pattern in core E27-30 is not as clear and is indicative of the influence of the STC at this site. In core E27-30 the subantarctic group dominates the fauna during stages 4, 6 and much of the period from stage 3 to the 2/1 boundary. The proportion of the subantarctic group at these times is greater than the value during the Holocene, indicating that the STC was north of its present position.

The subtropical group, generally low in abundance in this core, reaches a distinct maximum of some 12% at stage 5e (Fig. 7). This coincides with a peak in the transitional group and a strong drop in the subantarctic group. The subtropical group at this stage is characterised by the appearance of *Globigerinella aequilateralis*, a warm water species with a temperature tolerance of 11–30°C (Hemleben et al., 1989, p. 18). The influence of subtropical waters over the site at stage 5e is greater than during the Holocene, when *G. aequilateralis* is rare or absent and is due to a southward shift in the position of the STC. A less distinct warming occurs across the stage 1/2 boundary, shown in this case by an increase in the Transitional Group.

The position of the STC can also be traced using shifts in the ratio of sinistral coiling to total *N. pachyderma*. As shown by modern plankton studies in the Southeast Indian Ocean, these shifts occur at the STC (Hemleben et al., 1989, p. 184; Howard and Prell, 1992). The dextral form is more abundant in transitional waters to the north of the STC, while the sinistral form is dominant in sub-antarctic waters. In core E27-30 (Fig. 8) the sinistral form equals or even exceeds the dextral form in stages 4, 6 and stage 3 through to the 1/2 boundary, well exceeding relative abundances during the Holocene. These results confirm that the STC was to the north of its present position during these times. Using the 40% abundance of *N. pachyderma* (s) as an indicator of the location of the front, as suggested by Martinez (1994b), the STC was at, or even to the north, of the core site at these times. Low abundances of *N. pachyderma* (s) at stage 5e confirm the southward movement of the front. Comparison of abundances of *N. pachyderma* (s) throughout core E55-6 (Fig. 8) indicates that the STC did not move as far north as that site during the late Quaternary.

4.4. Benthic foraminiferal assemblages

Benthic species abundances are high in both cores. However, the dominant taxa in each core differ significantly. In core E55-6, *Cassidulina carinata, Globobulimina pacifica, Bulimina aculeata, B. striata, Oridorsalis tener* and *Hoegludina elegans*

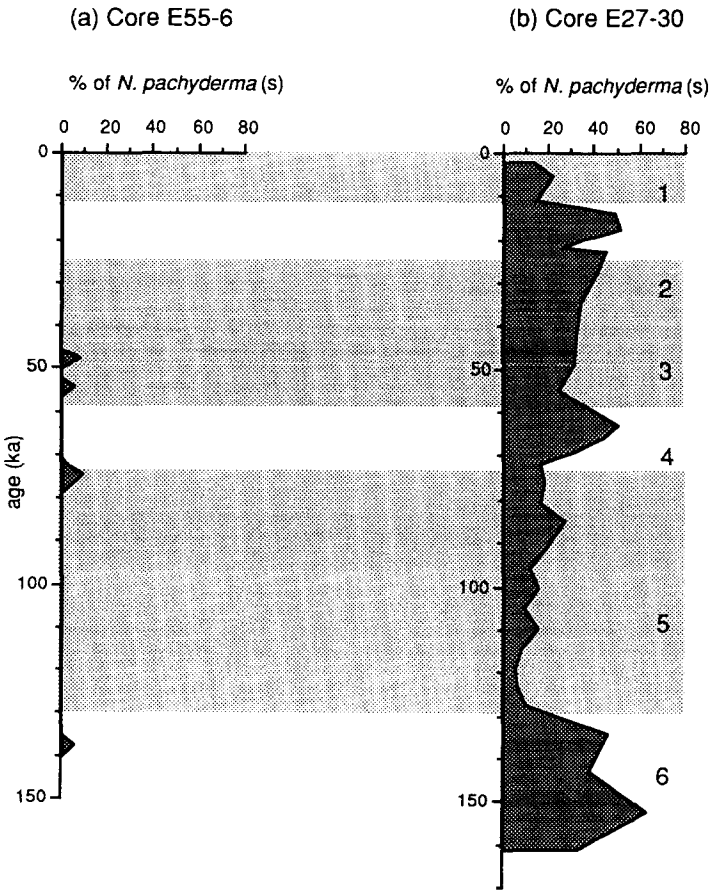

Fig. 8. Ratio of sinistral-coiling to total *N. pachyderma* in cores E55-6 and E27-30. Isotopic stages are indicated to the right of the figure, with interglacial periods shaded.

are the most abundant species (Fig. 9), comprising some 40–90% of the total fauna. Other important species include *Uvigerina* spp. (predominantly *U. peregrina*) and *Chilostomella oolina*. In contrast, the fauna in core E27-30 is dominated by *Epistominella exigua*, *U. peregrina*, *Globocassidulina subglobosa*, *Melonis barleeanum*, *Cibicidoides wuellerstorfi* and *Pullenia bulloides*, which together comprise some 40–60% of the total. (Fig. 10). Also relatively abundant in the core are *Pullenia* spp., *Trifarina bradyi* and *Fissurina* spp.

4.5. Benthic faunal characteristics and abundances

Benthic Foraminifera can be divided by their mode of living into epifaunal and infaunal taxa. Epifaunal taxa inhabit the top 0–1 cm of the sediment, while infaunal taxa can be divided into several groupings based on the depth range of sediment which they inhabit (Corliss and Chen, 1988; Rathburn and Corliss, 1994). Microhabitat preferences of benthic Foraminifera appear to be relatively consistent between different oceanic regions and to indicate adaptation to differing conditions of oxygen and organic carbon (Corliss, 1985, 1991; Mackensen et al., 1985; Sen Gupta and Machain-Castillo, 1993; Rathburn and Corliss, 1994).

Core E55-6 contains a number of infaunal species, such as *Globobulimina pacifica*, *Bulimina aculeata*, *B. striata*, *Chilostomella oolina* and *Uvigerina* spp. (predominantly *U. peregrina*). These taxa are predominantly deep infaunal (Corliss and Chen, 1988; Rathburn and Corliss, 1994), and have been interpreted as indicative of high organic carbon levels (Lutze and Coulbourn, 1984; Sen Gupta and Machain-Castillo, 1993; Rathburn and Corliss, 1994). In comparison, core E27-30 contains a much higher proportion of epifaunal species including *Epistominella exigua*, *Oridorsalis tener* (Corliss and Chen, 1988), together with abundant shallow infaunal species: *Globocassidulina subglobosa*, *Pullenia* spp., *Fissurina* spp., *U. peregrina* and *Melonis barleeanum* (Corliss and Chen, 1988; Rathburn and Corliss, 1994).

Carbon stable isotopes in Foraminifera are influenced by a number of factors, including pri-

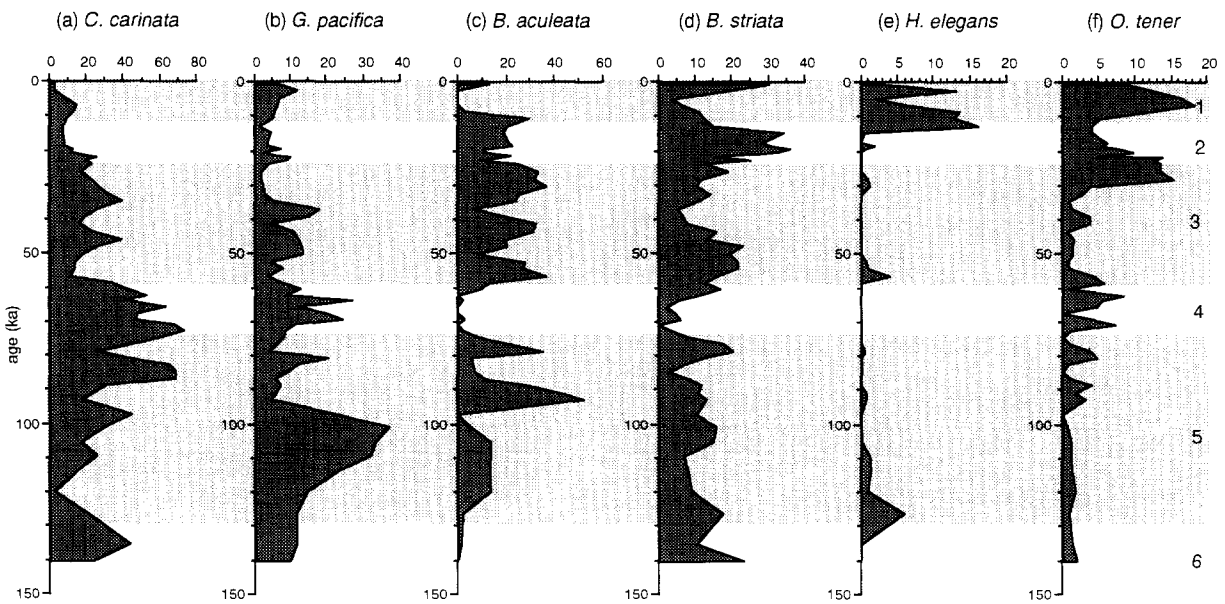

Fig. 9. Relative abundances of the main benthic Foraminifera in core E55-6: *Cassidulina carinata*, *Globobulimina pacifica*, *Bulimina aculeata*, *B. striata*, *Hoegludina elegans*, *Oridorsalis tener*. Isotopic stages are indicated to the right of the figure, with interglacial periods shaded.

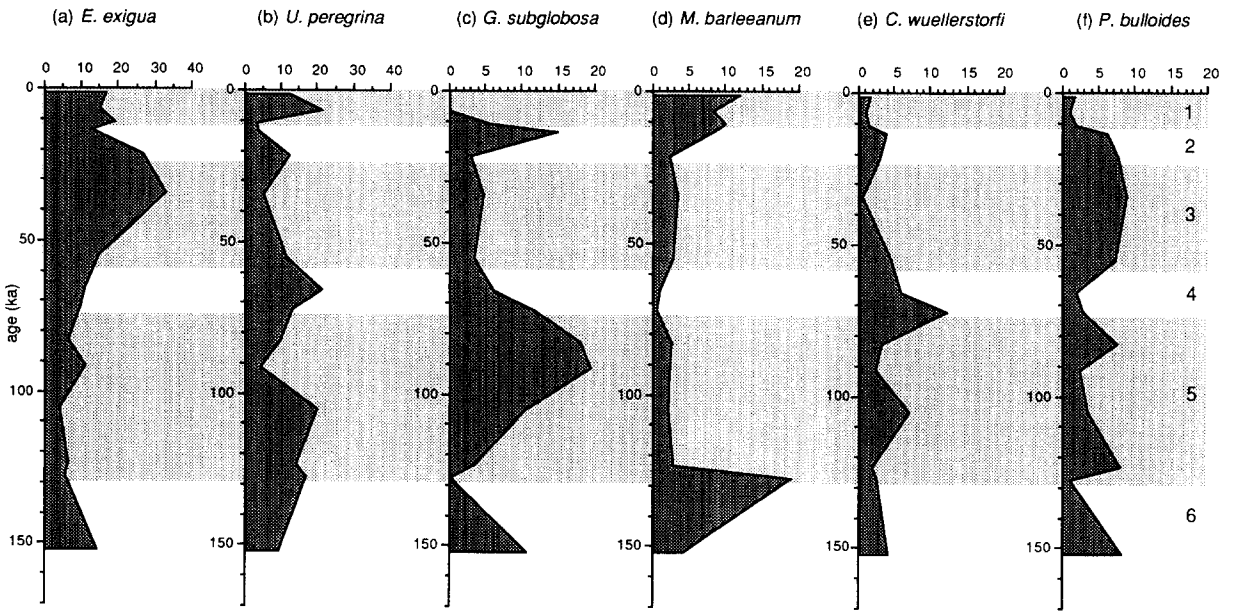

Fig. 10. Relative abundances of the main benthic Foraminifera in core E27-30: *Epistominella exigua*, *Uvigerina peregrina*, *Globocassidulina subglobosa*, *Melonis barleeanum*, *Cibicidoides wuellerstorfi*, *Pullenia bulloides*. Isotopic stages are indicated to the right of the figure, with interglacial periods shaded.

mary productivity, CO_2 and water-mass nutrient exchanges and vital effects, which differ between taxa, making $\delta^{13}C$ unreliable as a simple proxy for productivity. Nevertheless, $\delta^{13}C$ values of planktonic and benthic Foraminifera continue to be used as indicators of change in palaeoproductivity. The carbon stable-isotope record here is compared to the ratio of epifaunal:infaunal benthic Foraminifera and the benthic foraminiferal number, used as a proxy record of productivity (e.g. Herguera and Berger, 1991; Rathburn and Corliss, 1994). Both planktonic and benthic $\delta^{13}C$ records are available for core E55-6 (Fig. 11). For core E27-30 faunal records are compared with the planktonic $\delta^{13}C$ record only (Fig. 12).

No clear glacial/interglacial patterns are evident in core E55-6. Benthic abundances are highest in stages 2 and 3, peaking in stage 3. The abundance of productivity-related taxa in these stages suggests that productivity levels were higher in the region than at present. In contrast, benthic abundances in glacial stage 4 are very low and coincide with a change in faunal composition (Fig. 9). Stage 4 is dominated by *C. carinata* and *G. pacifica*, while other taxa, particularly *B. striata* and *B. aculeata*, show a distinct decrease in abundance. The contrast between these glacial stages indicates that there has been a significant difference in glacial productivity and/or dissolution regimes. Dissolution patterns are examined below.

Within core E27-30 there is a distinct transition in $\delta^{13}C$ values across the stage 5/6 boundary, followed by strong enrichment of $\delta^{13}C$ in stage 5e. The stage 1/2 boundary is characterised by a similar trend. These periods coincide with poleward excursions of the STC across the core site. At other times there is no clear correlation between proximity of the STC and the $\delta^{13}C$ record. Benthic foraminiferal abundances are highest in stage 3 and late in stage 2, at the time when the STC was located close to or over the core site. In contrast to core E55-6, core E27-30 does not show evidence of a strong decrease in benthic abundances during glacial stage 4.

4.6. Patterns of dissolution

Foraminiferal indices used to quantify dissolution include the proportion of planktonic frag-

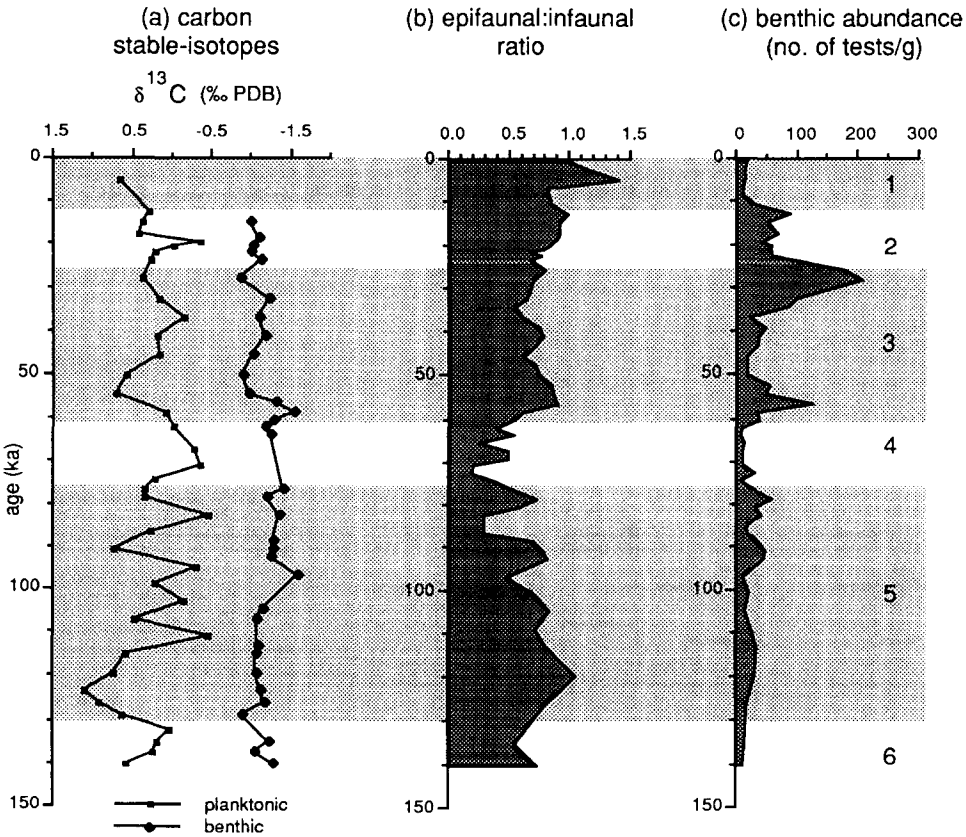

Fig. 11. Planktonic and benthic $\delta^{13}C$ compared with epifaunal: infaunal ratio and absolute abundance of benthic Foraminifera (number of tests per gram of sediment) in core E55-6. Isotopic stages are indicated to the right of the figure, with interglacial periods shaded.

ments to whole tests (as a percentage), the ratio of planktonic to benthic tests and a foraminiferal dissolution index (FDI) calculated using a seven rank system, based on the dissolution ranking of Vincent and Berger (1981).

Dissolution indicators for core E55-6 are compared in Fig. 13. The benthic:planktonic ratio shows little correlation with fragmentation, suggesting that downcore variations in the benthic:-planktonic ratio depend on factors other than dissolution. The FDI shows little change throughout the core, with only slight decreases during stages 2 and 4. The most significant dissolution is shown in stage 4 when the highest proportion of fragmentation coincides with the maximum in benthic:planktonic ratio and the minimum absolute abundance of planktonic Foraminifera.

The site of core E27-30 is some 600 m deeper than that of core E55-6. An increase in the overall dissolution level at this site is mirrored in both the proportion of fragmentation and the FDI (Fig. 14). The benthic:planktonic ratio (Fig. 14a) fluctuates at around 2% in comparison with that of core E55-6 which is around 4% (Fig. 13a). The ratio is highest in stage 2, with high levels through stages 4–2 and in stage 5. The FDI shows increased dissolution during glacial stages 2, 4 and also stage 6. The proportion of fragmentation is high in stage 2 and to a lesser extent in stage 4, but is low in stage 6.

Since the two cores are well above the lysocline, estimated at 4800 m in this region (Mallet and Heezen, 1977), some of the foraminiferal parameters used may not be sufficiently sensitive to esti-

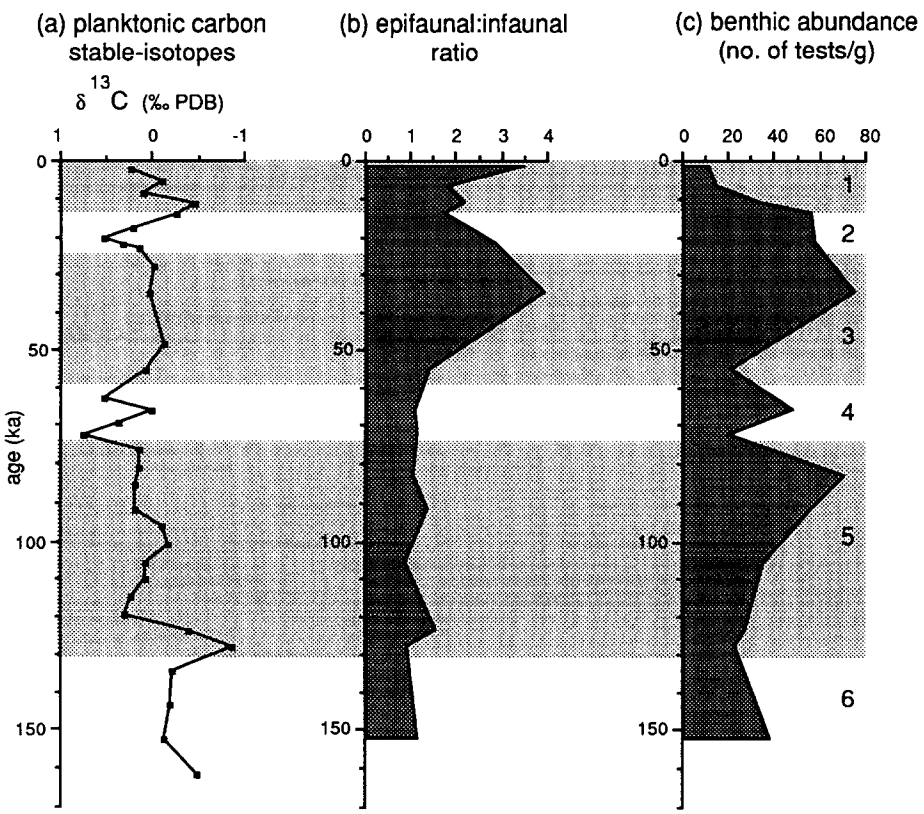

Fig. 12. Planktonic $\delta^{13}C$ compared with epifaunal: infaunal ratio and absolute abundance of benthic Foraminifera (number of tests per gram of sediment) in core E27-30. Isotopic stages are indicated to the right of the figure, with interglacial periods shaded.

mate dissolution. The lack of sensitivity of current foraminiferal dissolution indices in waters well above the lysocline has been pointed out by Le and Shackleton (1992) and more recently by Lohmann (1995). A comparison of foraminiferal indices with an ostracod dissolution index in the two cores examined here (Passlow, 1997-this issue) indicates that ostracods are more sensitive to dissolution at these shallower depths and probably reflect the extent of dissolution more accurately.

5. Discussion

5.1. Comparison with previous studies of the STC

The direction and timing of migrations of the STC recorded here are consistent with shifts documented in previous palaeoceanographic studies in the southern Indian and southeastern Indian Ocean (Prell et al., 1979; Morley, 1989; Howard and Prell, 1992; Francois et al., 1993). With only one core in this study located in the vicinity of the STC, it is not possible to constrain actual palaeolatitudes of the STC other than very broadly. Interpretation of the record in core E55-6 indicates that the STC did not move as far north as 39° S at any time during the late Quaternary. Within the Tasman Sea there is no evidence of migration of the STC as far north as DSDP Site 593 located at 40° 30' S (Nelson et al., 1993; Martinez, 1994b), which is consistent with the record in core E55-6.

Based on 40% abundance of *N. pachyderma* (s) as an indicator of the position of the front (Martinez, 1994b), the STC has moved at least as far north as 45° S during stages 6, 4 and 2, and was close to that latitude through much of stage 3. The record from core E36-23, located east of

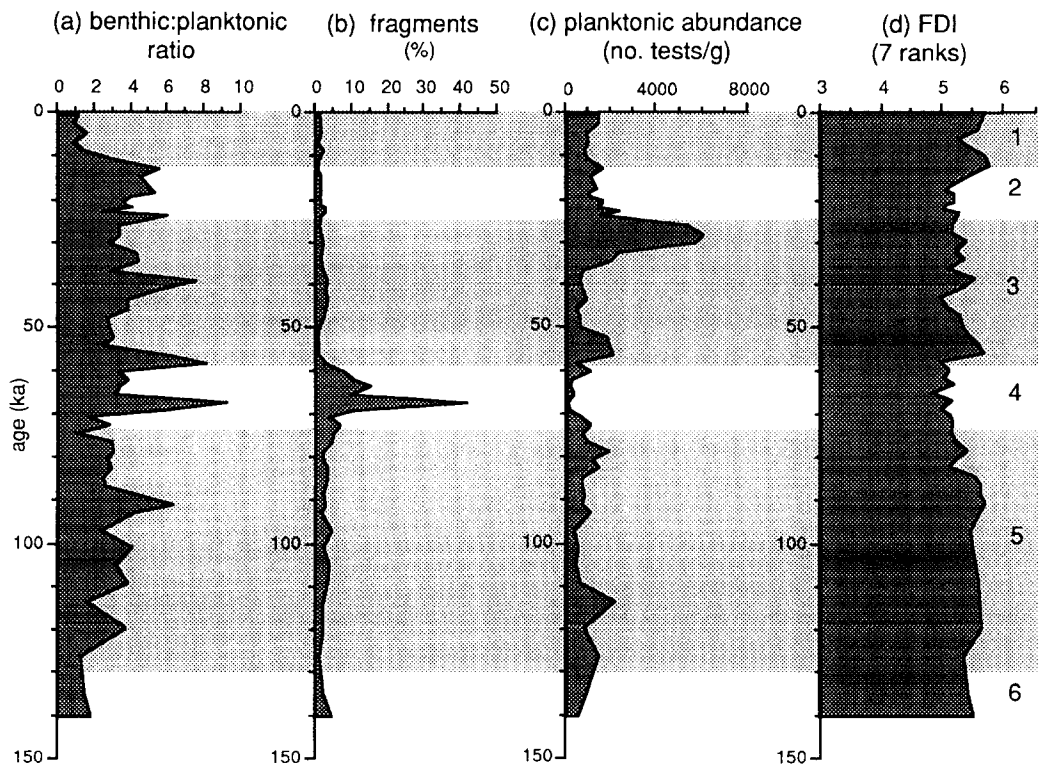

Fig. 13. Comparison of dissolution indicators in core E55-6: benthic: planktonic ratio; abundance of fragments to whole planktonic Foraminifera (%); absolute abundance of benthic Foraminifera (number of tests per gram of sediment) and foraminiferal dissolution index (FDI). Isotopic stages are indicated to the right of the figure, with interglacial periods shaded.

Tasmania at 43° S can also be used to provide a comparison (Martinez, 1994b). It should be noted though that the present path of the STC east of Tasmania curves northward (Fig. 1). Results from core E36-23 show that the STC migrated slightly north of 43° S during stages 6, 10 and 12 (Martinez, 1994b). This is consistent with the peak abundance of *N. pachyderma* (s) in core E27-30 at stage 6 and suggests that the STC migrated at least 2° north of its present position at that time. Abundances of *N. pachyderma* (s) in core E27-30 are not as high in subsequent glacial stages, suggesting that the STC was located at or slightly north of 45° S at these times.

The results examined here provide a preliminary assessment of the record of the STC in the region south of Tasmania. To better define the extent of movements of the STC requires a study based on a transect of cores across the present zone of the STC. Proper delineation of the front also requires analysis based on temperature data derived from planktonic foraminiferal assemblages using data processing, such as the modern analogue technique.

5.2. *Benthic productivity and the influence of the STC*

The records of benthic foraminiferal assemblages and patterns of dissolution differ considerably in the two cores. These differences are greater than might be expected from cores located within the same low-nutrient water mass. The nature of circulation south of Australia is such that water properties at depth are relatively homogeneous. There is no evidence from modern water-mass data of significant differences in water temperature or productivity levels which might account for the

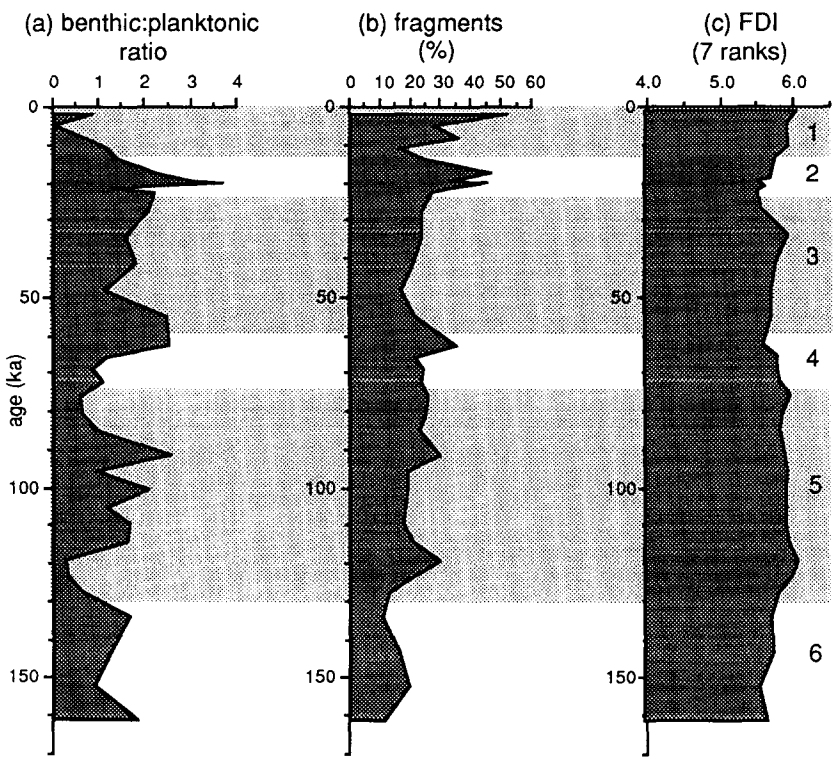

Fig. 14. Comparison of dissolution indicators in core E27-30: benthic: planktonic ratio; abundance of fragments to whole planktonic Foraminifera (%) and foraminiferal dissolution index (FDI). Isotopic stages are indicated to the right of the figure, with interglacial periods shaded.

very different benthic foraminiferal faunas. However, the sites of the two cores differ significantly in their surface waters. Core E27-30 is located adjacent to the STC and has higher levels of surface productivity due to seasonal phytoplankton blooms associated with the front. In the region of core E55-6, and along much of the southern margin of the continent, modern productivity levels are very low.

The importance of productivity in influencing the distribution of benthic Foraminifera has become increasingly clear in recent years (Lutze and Coulbourn, 1984; Corliss and Chen, 1988; Corliss and Emerson, 1990; Loubere, 1991; Sen Gupta and Machain-Castillo, 1993). A recent study of benthic Foraminifera from the Sulu Sea, where bottom water temperatures, salinity and oxygen levels are all uniform, indicates that differences in the faunas can be linked to variations in the organic carbon content of the sediments (Rathburn and Corliss, 1994). The latter study confirms the contention that productivity levels provide the major control over the distribution of many of the taxa which have been previously linked with both high productivity and low-oxygen conditions (Sen Gupta and Machain-Castillo, 1993).

Studies of modern seasonal phytodetrital deposits in the North Atlantic have shown that a small group of taxa, dominated by *Epistominella exigua* and *Alabaminella weddellensis*, is adapted to feeding directly on these seasonal inputs (Gooday, 1986; Gooday and Lambshead, 1989; Gooday and Turley, 1990). Based on the association of *E. exigua* with phytodetritus in the modern environment, Smart et al. (1994) have suggested that this species may be an indicator of palaeoproductivity.

Other taxa that have been recorded in associa-

tion with these phytoplankton feeders include *Cibicidoides wuellerstorfi*, *Globocassidulina subglobosa*, *Chilostomella* sp. and *Melonis barleeanum* (Caralp, 1984, 1989; Gooday, 1988; Gooday and Turley, 1990; Gooday et al., 1992). These taxa take advantage of the more degraded organic material available, rather than feeding directly on phytodetritus (Caralp, 1989). While these taxa are not limited to areas with seasonal phytoplankton input, they are commonly more abundant in the sediment below phytoplankton snow. The remaining infaunal population can also benefit from the increased levels of organic material resulting in increased population numbers overall (Gooday, 1988).

In core E27-30 *E. exigua* is one of the most abundant taxa present. Other taxa found in abundance include a number of the species which have been recorded in association with phytodetrital input: *C. wuellerstorfi*, *Globocassidulina subglobosa* and *Melonis barleeanum*. These taxa, together with *E. exigua*, are more abundant at times when the STC is located over the site: stages 6, 4 and stage 3 through to the stage 1/2 transition (Fig. 15). In comparison, these taxa are rare to absent in core E55-6.

The data here indicate that the benthic faunal record in core E27-30 has been strongly influenced by seasonal phytoplankton production associated with the STC. The distribution of *E. exigua*, in conjunction with other productivity-related benthic taxa, confirms that the species can be used to provide a record of high seasonal phytoplankton productivity (Smart et al., 1994; Thomas et al., 1995). Abundances of *E. exigua* and *A. weddellensis* have been used to trace phytoplankton productivity associated with the Polar Front in the northeastern Atlantic (Thomas et al., 1995).

5.3. Dissolution and productivity links

The most obvious dissolution event in core E55-6 occurs in stage 4 and is marked by a distinct change in both benthic faunal and dissolution records, compared to those in glacial stage 2. The reasons for the dissolution peak in this core are unclear. A long-term trend of increasing carbonate preservation over the past 500,000 yr has been observed in the Southern Ocean and in the Tasman Sea (Howard and Prell, 1994; Martinez, 1994a). It may be that this trend accounts for differences between glacial stages. With little of stage 6 represented in the core it is not possible to compare earlier glacial cycles or establish longer-term trends.

The absence of a similar pattern in core E27-30 suggests either that the pattern observed in core E55-6 is due to local input, such as increased upwelling, or that the impact of the STC has obscured other dissolution trends in core E27-30. The high organic carbon input caused by the STC is likely to increase the level of dissolution and, in fact, increased dissolution levels are associated with the presence of the STC over the site.

The abundance of benthic Foraminifera in core E55-6 decreases overall in stage 4, but this is not the case for all taxa. The fauna in stage 4 comprises infaunal taxa and is dominated by two species, *Cassidulina carinata* and *Globobulimina pacifica*. Studies of modern benthic Foraminifera have shown that some thin-shelled taxa, including *Globobulimina* spp. are able to move deeper in the sediment in conditions of high to extreme corrosivity, such as in sediments below the carbonate compensation depth (Rathburn and Corliss, 1994; Rathburn et al., 1996).

The ability of some infaunal benthic Foraminifera to inhabit different depths within the substrate allows these taxa to take advantage of increased levels of organic carbon at depth in the sediments (Griggs et al., 1969; Corliss and Chen, 1988; Corliss and Emerson, 1990; Rathburn and Corliss, 1994; Rathburn et al., 1996). It is possible that the fauna recorded during stage 4 in core E55-6 developed as a consequence of high corrosivity together with high levels of organic carbon in the sediment. Planktonic and benthic $\delta^{13}C$ values during this stage are consistent with increased levels of productivity. The cause of this increase is not clear, however.

5.4. Implications for palaeoceanographic studies

The differences between these two cores indicate the extent to which frontal structures can influence palaeoceanographic records. The record of the

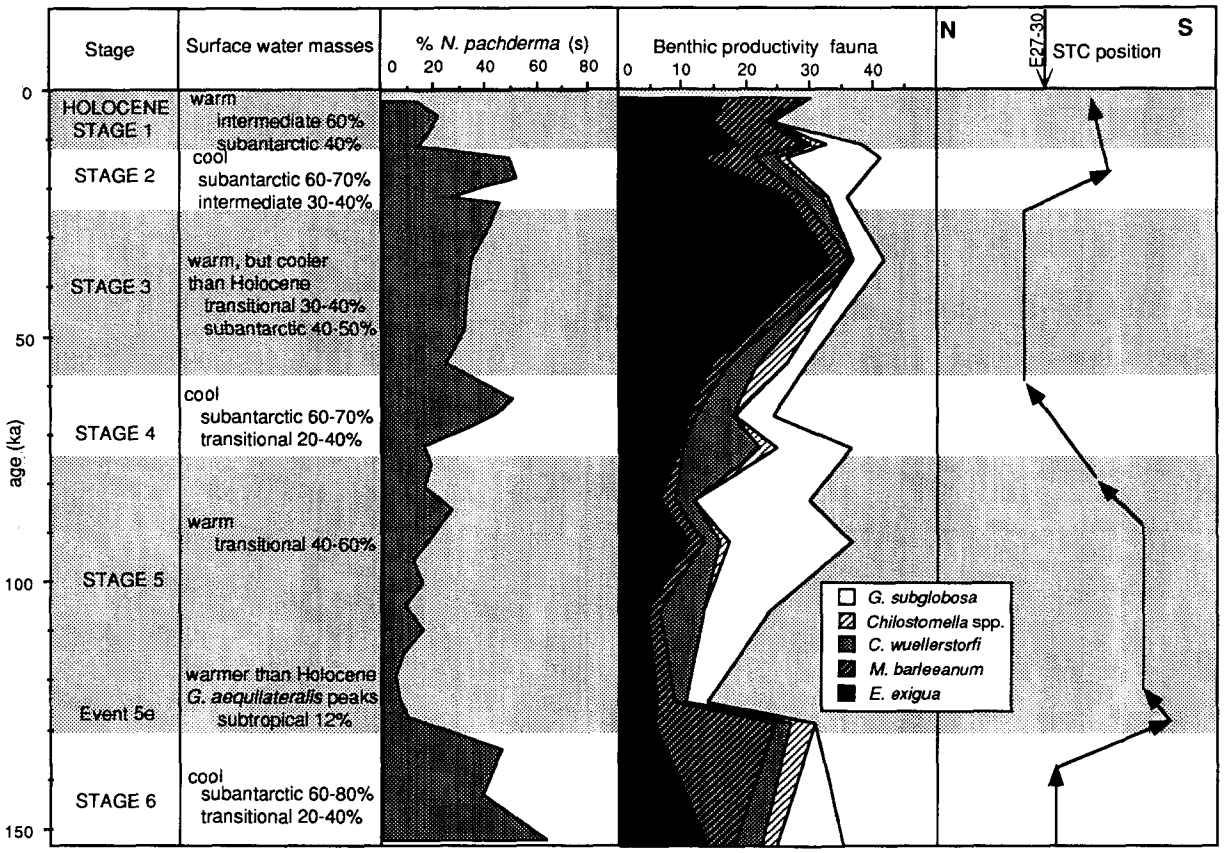

Fig. 15. Summary of evidence of movements of the STC through the late Quaternary at core site E27-30, based on surface water-mass interpretations, ratio of sinistral-coiling to total *N. pachyderma* and benthic Foraminifera associated with phytodetrital influx (see text for discussion). The position of core E27-30, relative to the STC, is indicated by the arrow. Interglacial stages are shaded.

STC is apparent not only in the planktonic record of core E27-30, but has also been a major influence on the benthic foraminiferal record. Other recent Southern Ocean studies have found evidence of the influence of productivity associated with frontal structures (Francois et al., 1993; Mackensen et al., 1993). The study by Mackensen et al. (1993) showed that $\delta^{13}C$ values in *C. wuellerstorfi* may in fact be lowered by regional surface production and organic carbon flux changes. Given the importance of the Southern Ocean in global climate regulation and, in particular, the interest in determining glacial/interglacial changes in deep- and bottom-water production, it is essential that the impact of frontal structures be recognised.

6. Conclusions

Comparisons between two cores located in the southeast Indian Ocean off southeastern Australia provide a record of palaeoceanographic changes through the late Quaternary. Planktonic foraminiferal assemblages and the ratio of sinistral-coiling to total *N. pachyderma* are used to record variations in surface water masses over the location of core E27-30, south of Tasmania. These changes in surface water masses are interpreted as a record of movement of the Subtropical Convergence over the site.

The record from core E27-30 indicates that the STC has been located north of its present location

through much of the late Quaternary, particularly in stage 6 and stages 2–4. Poleward excursions of the STC occurred during stage 5e and the Holocene, resulting in the presence of warmer surface waters over the site. Movements of the STC identified here are consistent in timing and direction with those identified in other core studies in the southern Indian and southeastern Indian Ocean.

This study provides limited control on the palaeolatitude of the STC. The record in core E55-6 indicates that the front never migrated as far north as 39° S during the late Quaternary. The maximum northward movement recorded occurred during stage 6, when the front moved at least 2° north of its present position and possibly more. The position of the STC in stages 2–4 was at or slightly north of 45° S.

Benthic foraminiferal faunas and abundances in core E27-30 can be linked to variations in surface productivity associated with movements of the Subtropical Convergence. The abundance of the species *Epistominella exigua*, known to feed directly on phytoplankton detritus in the modern deep-sea (Gooday, 1986; Gooday and Lambshead, 1989; Gooday and Turley, 1990) correlates with periods when the STC was close to the core site. Overall benthic abundances are also higher at these times, indicating that phytodetrital material has played a significant role in benthic productivity at this site.

Dissolution records in the two cores differ. A significant event occurs during stage 4 of core E55-6, but is not evident in core E27-30. The reasons for the differences in the core records are not clear, but may be related to local effects, including the influence of the STC on the site of core E27-30. Comparison of these two core records emphasises the importance of frontal structures in influencing palaeoceanographic records in the southeast Indian Ocean–Southern Ocean region and the need for the record of the STC to be better defined.

Acknowledgements

We would like to express our sincere gratitude to Patrick De Deckker for providing extensive support and encouragement throughout the development of this work and for providing financial and other assistance to enable W.P to visit Australia. Dennis Cassidy, former curator at the Antarctic Core Facility, University of Florida, generously assisted with sampling of cores and provided additional information; Joe Cali from the Research School of Earth Sciences, ANU assisted with the stable-isotope analyses. We would also like to thank Tony Rathburn, Leanne Armand and, particularly, Mike Ayress for discussion of aspects of this paper. Comments by Giles Bareille and an anonymous reviewer improved the paper considerably. V.P. would like to acknowledge Sandy Radke of the Bureau of Resource Sciences for her encouragement to complete this paper. Much of this work was carried out by V.P. as part of a Ph.D. study, funded by an Australian Postgraduate Research Award at the Australian National University.

References

Almond, D., McGowran, B. and Qianyu Li, 1993. Late Quaternary foraminiferal record from the Great Australian Bight and its environmental significance. Mem. Assoc. Australas. Palaeontol., 15: 417–428.

Bé, A.W.H., 1977. An ecological, zoogeographic and taxonomic review of Recent planktonic Foraminifera. In: A.T.S. Ramsay (Editor), Oceanic Micropalaeontology Volume 1. Academic Press, London, pp. 1–100.

Bé, A.W.H. and Tolderlund, D.S., 1971. Distribution and ecology of living planktonic foraminifera in surface waters of the Atlantic and Indian Oceans. In: B.M. Funnell and Riedel, W.R. (Editors), Micropalaeontology of Oceans. Cambridge Univ. Press, New York, pp. 105–149.

Boreen, T., James, N., Wilson, C. and Heggie, D., 1993. Surficial cool-water carbonate sediments on the Otway continental margin, southeastern Australia. Mar. Geol., 112: 35–56.

Boreen, T.D. and James, N.P., 1993. Holocene sediment dynamics on a cool-water carbonate shelf: Otway, Southeastern Australia. J. Sediment. Geol., 63: 574–588.

Burns, D.A., 1975. The abundance and species composition of nannofossil assemblages in sediments from continental shelf to offshore basin, western Tasman Sea. Deep-Sea Res., 22: 425–431.

Caralp, M.-H., 1984. Impact de matière organique dans des zones de forte productivité sur certains foraminifères benthiques. Oceanol. Acta, 7: 509–516.

Caralp, M.-H., 1989. Abundance of *Bulimina exilis* and *Melonis*

Neogloboquadrina dutertrei	*Neogloboquadrina pachyderma (s)*	*Neogloboquadrina pachyderma (d)*	*Pulleniatina obliquiloculata*	*Orbulina universa*	*Globigerinella aequilateralis*	*Globigerinita glutinata*	*Globorotalia crassaformis*	*Globigerina digitata*	*Globigerinoides conglobatus*	other	no. fragments
10	2	63	0	1	3	9	0	0	0	66	55
12	0	51	0	3	1	64	1	1	0	1	81
1	0	22	0	5	11	39	2	0	0	2	43
2	1	30	0	5	3	44	1	0	0	17	36
1	0	20	0	6	2	30	1	0	0	17	57
3	0	30	0	8	0	29	0	0	0	20	45
2	0	21	0	15	3	33	0	0	0	18	34
0	0	17	0	0	0	51	0	0	1	6	47
0	0	19	0	0	0	62	0	0	0	11	63
0	0	8	0	0	0	30	0	0	0	9	52
0	0	12	0	0	1	47	0	0	0	10	39
3	0	11	0	0	0	44	0	0	0	10	66
3	0	7	0	0	0	40	0	0	0	8	45
2	0	8	0	0	0	57	0	0	0	9	102
6	0	9	0	0	0	36	0	0	0	20	132
0	19	2	0	0	0	29	0	0	0	17	58
9	0	14	0	0	0	31	0	1	0	18	42
14	0	19	0	9	0	42	0	0	0	22	66
10	0	24	0	5	0	39	0	0	0	25	81
7	0	21	0	4	0	37	0	0	0	15	64
6	0	13	0	1	0	49	0	0	0	14	58
2	0	19	0	0	0	53	0	1	0	20	65
9	0	5	0	4	0	48	0	5	0	16	162
2	0	3	0	1	0	24	0	0	0	20	94
1	0	20	0	1	0	24	0	0	0	20	79
0	0	16	0	1	0	9	0	0	0	18	68
5	3	32	1	4	1	63	0	0	0	30	153
7	0	20	0	0	0	59	0	0	0	15	43
1	0	18	0	4	0	99	0	0	0	25	45
4	2	43	0	8	0	58	0	0	0	30	65
3	0	31	0	3	1	99	0	0	0	12	53
4	0	10	0	1	0	43	1	0	0	18	124
3	0	23	0	1	0	58	0	0	0	20	58
5	0	24	0	1	0	42	0	0	0	18	300

Neogloboquadrina dutertrei	*Neogloboquadrina pachyderma (s)*	*Neogloboquadrina pachyderma (d)*	*Pulleniatina obliquiloculata*	*Orbulina universa*	*Globigerinella aequilateralis*	*Globigerinita glutinata*	*Globorotalia crassaformis*	*Globigerina digitata*	*Globigerinoides conglobatus*	other	no. fragments
4	0	22	0	1	0	67	0	0	0	18	655
3	0	12	0	0	0	37	0	0	0	23	334
3	0	10	0	0	0	78	0	0	0	15	1600
4	0	26	0	3	0	54	0	0	0	30	340
1	0	45	0	0	0	48	0	0	0	14	102
7	1	49	0	0	0	109	2	0	0	15	250
6	3	30	0	0	0	55	0	0	0	18	158
12	2	35	0	0	0	93	0	0	0	40	245
0	0	8	0	2	0	96	3	0	0	14	79
0	0	6	0	2	1	48	0	0	0	18	621
5	0	15	0	5	0	47	0	0	0	15	104
4	0	18	0	0	0	40	0	1	0	20	134
1	0	10	0	5	0	57	1	0	0	18	118
4	0	25	0	6	1	28	0	0	0	25	90
8	0	23	0	5	4	24	0	0	0	16	102
2	0	8	0	5	0	69	0	0	0	18	67
2	0	25	0	3	0	2	0	1	0	30	130
2	0	34	0	0	0	35	0	0	0	22	82
2	0	35	0	0	0	14	0	0	0	16	122
2	0	13	0	0	0	21	0	0	0	12	97
4	0	31	0	0	1	50	0	0	0	42	140
8	0	34	0	2	2	40	0	0	0	22	83
4	0	17	0	0	0	36	0	0	0	13	24
9	1	38	0	0	0	99	0	0	0	21	130
2	0	13	0	0	1	21	0	0	0	18	75
4	0	7	0	1	0	28	0	0	0	18	70
2	1	19	0	0	0	36	0	0	0	15	120
1	0	16	0	0	1	48	0	0	0	20	170

Appendix A

Core E55-6 planktonic foraminiferal counts

core depth (cm)	planktonic total	*Globorotalia truncatulinoides (s)*	*Globorotalia truncatulinoides (d)*	*Globorotalia inflata*	*Globorotalia scitula*	*Globorotalia hirsuta*	*Globigerina bulloides*	*Globigerina falconensis*	*Globigerina quinqueloba*	*Globigerinoides ruber*
2	449	51	0	138	8	2	19	4	13	32
5	463	42	0	152	9	1	39	28	9	31
10	289	29	0	92	7	0	27	19	4	17
15	290	0	34	56	4	1	26	8	0	49
20	264	0	32	88	6	8	16	3	8	20
25	317	0	68	105	3	3	18	5	3	13
30	605	174	0	221	11	5	31	10	2	48
35	274	78	0	36	3	1	42	4	22	1
40	330	47	0	35	0	3	71	2	62	0
45	263	32	0	36	1	0	63	0	71	2
50	293	44	0	43	1	0	60	3	60	3
55	394	73	0	52	1	0	75	4	110	1
60	280	60	0	25	1	1	53	0	77	0
65	344	49	0	32	1	0	88	4	80	2
70	433	53	0	61	2	1	99	1	131	1
75	322	63	47	1	0	63	4	7	3	8
80	350	44	0	69	0	4	104	2	43	0
85	374	55	0	42	4	3	76	11	60	0
90	398	76	0	85	2	3	67	7	45	1
95	321	40	0	57	0	0	89	1	38	0
100	293	47	0	60	1	1	57	2	37	0
105	319	46	0	30	2	0	37	0	101	1
110	442	58	0	165	8	4	61	4	47	3
115	303	55	0	79	11	4	42	5	43	11
120	228	10	0	28	8	0	45	3	61	1
125	218	20	0	39	7	0	17	2	85	0
130	711	52	2	180	37	1	167	3	121	2
135	322	37	1	56	14	0	65	4	31	6
140	544	87	1	136	4	4	67	4	84	3
145	572	129	2	141	8	0	73	3	60	5
150	431	80	2	119	4	2	30	6	25	10
155	389	21	0	58	7	0	116	1	105	0
160	445	40	1	64	11	0	96	0	124	0
165	278	22	1	25	0	0	74	3	60	0

core depth (cm)	planktonic total	*Globorotalia truncatulinoides (s)*	*Globorotalia truncatulinoides (d)*	*Globorotalia inflata*	*Globorotalia scitula*	*Globorotalia hirsuta*	*Globigerina bulloides*	*Globigerina falconensis*	*Globigerina quinqueloba*	*Globigerinoides ruber*
170	415	44	0	68	9	0	96	1	73	0
175	331	19	1	27	8	0	86	0	104	0
180	352	39	0	44	10	0	60	0	89	0
185	312	19	0	22	16	0	56	0	77	0
190	252	10	1	18	3	0	49	0	59	0
195	378	25	2	19	4	1	41	0	75	0
200	301	16	1	32	10	0	64	0	61	0
205	526	47	0	92	8	0	97	7	82	4
210	370	71	0	72	3	8	32	20	24	12
215	252	44	1	42	2	3	42	9	26	4
220	322	25	0	49	4	0	96	3	56	0
225	382	76	1	105	12	0	47	3	49	2
230	414	105	2	112	14	1	60	2	22	1
235	368	71	2	117	12	0	38	3	30	3
240	352	91	0	96	15	0	36	6	14	10
245	390	90	2	106	11	3	20	23	14	15
255	297	75	0	60	22	0	50	4	18	0
265	395	105	0	60	21	0	51	2	54	3
275	321	79	0	60	23	0	43	0	34	4
285	301	70	0	88	14	2	31	1	37	6
295	575	174	4	132	19	4	62	4	37	5
310	382	96	4	97	3	7	28	8	17	9
330	262	34	0	63	3	5	34	17	15	14
350	467	58	1	50	21	0	90	15	53	4
360	316	44	0	118	1	0	74	4	20	0
370	290	32	0	103	4	1	42	6	31	10
380	371	51	0	132	7	0	56	9	37	6
390	364	59	0	112	15	2	47	5	16	17

Globigerinoides ruber	*Neogloboquadrina dutertrei*	*Neogloboquadrina pachyderma (s)*	*Neogloboquadrina pachyderma (d)*	*Orbulina universa*
0	1	57	101	7
1	0	21	142	12
1	1	23	85	11
2	3	32	142	10
1	6	15	90	8
1	1	53	56	2
1	0	46	43	2
0	0	129	129	0
0	5	21	32	0
0	0	24	44	1
0	0	23	64	3
0	1	23	28	2
0	0	28	40	2
0	0	45	87	3
0	0	31	66	1
0	0	34	73	3
0	1	15	47	0
0	1	20	31	0
0	1	30	30	0
0	0	48	62	0
0	2	37	79	2
0	2	19	99	0
0	5	26	118	2
0	0	20	103	2
1	1	29	80	1
0	0	15	66	3
0	0	13	99	2
0	8	18	99	1
0	3	12	122	1
0	5	16	88	2
1	0	11	120	5
0	1	10	183	11
6	1	7	102	15

Globigerinella aequilateralis	*Globigerinita glutinata*	other	no. fragments
0	21	4	152
0	11	3	383
1	11	2	128
0	18	2	258
0	18	3	65
0	26	3	113
0	26	0	275
0	41	1	70
0	13	1	165
0	3	1	290
0	6	2	185
0	10	6	135
0	9	6	105
0	18	0	96
0	10	0	89
0	13	2	74
0	15	3	87
0	7	2	40
0	12	0	174
0	18	1	94
0	9	1	116
0	10	1	115
0	11	2	118
0	15	2	106
0	20	1	96
0	11	0	130
0	11	3	76
0	21	2	78
0	10	0	77
0	7	1	63
0	7	3	82
0	11	1	158
9	13	2	87

Globigerinoides ruber	*Neogloboquadrina dutertrei*	*Neogloboquadrina pachyderma (s)*	*Neogloboquadrina pachyderma (d)*	*Orbulina universa*
1	2	11	103	18
0	3	27	32	2
0	1	35	57	4
0	1	43	25	1
0	3	23	49	0
0	1	20	58	3

Globigerinella aequilateralis	*Globigerinita glutinata*	other	no. fragments
4	27	0	47
0	21	1	36
0	15	1	60
0	14	0	80
0	17	1	41
0	15	2	16

Appendix B

Core E27-30 planktonic foraminiferal counts

core depth (cm)	planktonic total	*Globorotalia truncatulinoides (s)*	*Globorotalia truncatulinoides (d)*	*Globorotalia inflata*	*Globorotalia scitula*	*Globorotalia hirsuta*	*Globigerina bulloides*	*Globigerina falconensis*	*Globigerina rubescens*	*Globigerina quinqueloba*
1	325	8	0	34	1	0	65	0	0	26
9.5	354	16	0	77	1	0	65	0	0	5
20	333	14	0	84	1	0	97	0	0	2
30	458	19	0	95	0	1	130	2	0	2
40	344	14	0	92	1	0	89	0	0	7
50	359	16	1	54	4	0	120	3	0	19
60	316	11	1	45	2	0	120	2	0	17
70	430	5	0	30	5	0	42	3	0	45
75	332	17	2	80	2	1	154	0	0	4
80	354	13	0	50	0	0	216	0	0	2
90	385	12	0	69	1	0	200	2	0	3
98	362	18	0	61	0	2	203	0	0	8
110	336	14	0	51	1	0	174	0	0	11
120	314	17	0	50	0	0	87	0	0	7
130	331	15	2	64	1	1	136	0	0	4
140	363	12	0	58	0	0	165	0	0	3
150	322	24	1	68	1	1	143	0	0	3
160	323	18	2	80	2	0	158	0	0	2
180	319	20	0	45	1	0	177	0	0	3
190	346	11	0	64	1	0	139	0	0	2
200	359	14	2	61	1	0	145	0	0	6
210	367	16	0	74	3	0	133	1	0	9
220	337	19	1	55	0	0	94	1	0	3
230	319	13	0	51	1	0	108	0	0	4
240	318	20	0	46	1	0	106	1	0	11
280	310	4	0	105	2	0	103	0	0	1
290	324	15	1	81	1	0	97	0	0	1
300	336	17	0	63	1	0	103	0	0	3
310	347	25	0	60	1	1	110	2	0	0
320	300	24	1	55	0	0	100	0	0	1
330	311	28	1	44	1	0	87	0	0	3
340	376	29	0	57	1	0	68	2	0	2
350	329	18	3	85	0	1	61	2	0	3

core depth (cm)	planktonic total	*Globorotalia truncatulinoides (s)*	*Globorotalia truncatulinoides (d)*	*Globorotalia inflata*	*Globorotalia scitula*	*Globorotalia hirsuta*	*Globigerina bulloides*	*Globigerina falconensis*	*Globigerina rubescens*	*Globigerina quinqueloba*
360	324	15	3	46	1	0	90	6	2	7
370	303	14	3	61	3	1	128	0	0	7
380	318	28	0	38	0	0	135	0	0	4
390	330	13	0	39	0	0	191	0	0	3
400	324	16	1	51	1	0	156	0	0	6
410	308	18	0	49	0	1	128	0	0	13

barleeanum: relationship to the quality of marine organic matter. Geo-Mar. Lett., 9: 37–43.

Chivas, A.R., De Deckker, P., Cali, J.A., Chapman, A., Kiss, E. and Shelley, J.M.G., 1993. Coupled stable-isotope and trace-element measurements of lacustrine carbonates as paleoclimatic indicators. In: P.K. Swart, K.C. Lohmann, J. McKenzie and S. Savin (Editors), Climate Change in Continental Isotopic Records. Am. Geophys. Union Monogr., 78: 113–121.

Corliss, B.H., 1985. Microhabitats of benthic foraminifera within deep-sea sediments. Nature, 314: 435–438.

Corliss, B.H., 1991. Morphology and microhabitat preferences of benthic foraminifera from the northwest Atlantic Ocean. Mar. Micropaleontol., 17: 195–236.

Corliss, B.H. and Chen, C., 1988. Morphotype patterns of Norwegian Sea deep-sea benthic foraminifera and ecological implications. Geology, 16: 716–719.

Corliss, B.H. and Emerson, S., 1990. Distribution of Rose Bengal stained deep-sea benthic foraminifera from the Nova Scotian continental margin and Gulf of Maine. Deep-Sea Res., 37: 381–400.

Cresswell, G.R., Golding, T.J. and Boland, F.M., 1978. A buoy and ship examination of the Subtropical Convergence south of Western Australia. J. Phys. Oceanogr., 8: 315–320.

Deacon, G.E.R., 1937. The Hydrology of the Southern Ocean. Cambridge Univ. Press, 124 pp.

Division of Fisheries and Oceanography, 1962. Oceanographical Observations in the Indian Ocean in 1960. HMAS *Diamantina* Cruise Dm1/60. CSIRO Division of Fisheries and Oceanography, Oceanographical Rep., 2, 128 pp.

Division of Fisheries and Oceanography, 1966. Oceanographical Observations in the Indian and Pacific Oceans in 1961. HMAS *Gascoyne* Cruise G2/61. CSIRO Division of Fisheries and Oceanography, Oceanographical Cruise Rep., 10, 165 pp.

Division of Fisheries and Oceanography, 1967a. Oceanographical Observations in the Indian Ocean in 1963. HMAS *Gascoyne* Cruise G 2/63. CSIRO Division of Fisheries and Oceanography, Oceanographical Cruise Rep., 22, 51 pp.

Division of Fisheries and Oceanography, 1967b. Oceanographical Observations in the Indian and Pacific Oceans in 1964. HMAS *Gascoyne* Cruise G3/64. CSIRO Division of Fisheries and Oceanography, Oceanographical Cruise Rep., 35, 40 pp.

Drapala, V., 1993. The use of ostracods in detecting fine grained turbidites in deep sea cores. In: K.G. McKenzie and P.J. Jones (Editors), Ostracoda in the Earth and Life Sciences. Balkema, Rotterdam, pp. 559–568.

Edwards, R.J. and Emery, W.J., 1982. Australasian Southern Ocean frontal structure during Summer 1976–77. Aust. J. Mar. Freshwater Res., 33: 3–22.

Exon, N.F., Stratton, J.P., Reynolds, H.W. and Tindall, C., 1989. Sedimentological Analyses from Deepsea Cores Taken Off Southwest Victoria, and Western and Southern Tasmania. Bur. Miner. Resour., Geol. Geophys. Record 1989/5, 38 pp.

Exon, N.F., Lee, C.S., Felton, E.A., Heggie, D., McKirdy, D., Penney, C., Shafik, S., Stephenson, A. and Wilson, C., 1992. BMR Cruise 67: Otway Basin and West Tasmanian Sampling. Bur. Miner. Resour., Geol. Geophys. Rep., 306, 171 pp.

Exon, N.F., Hill, P.J., Royer, J.-Y., Muller, D., Whitmore, G., Belten, D., Dutkiewicz, A., Ramel, C., Rollet, N., Wellington, A., 1994, Tasmante Swath-Mapping and Reflection Seismic Cruise off Tasmania Using R.V. L'Atalante. Australian Geological Survey Organisation, Record 1994/68, 72 pp.

Fine, R.A., 1993. Circulation of Antarctic Intermediate Water in the South Indian Ocean. Deep-Sea Res., 40: 2021–2042.

Francois, R., Bacon, M., Altabet, M.A. and Labeyrie, L.D., 1993. Glacial/interglacial changes in sediment rain rate in the SW Indian sector of Subantarctic waters as recorded by ^{230}Th, ^{231}Pa, U, and $\delta^{15}N$. Paleoceanography, 8: 611–629.

Francois, R., Altabet, M.A., Goericke, R., McCorckle, D.C., Brunet, C. and Poisson, A., 1994. Changes in the $\delta^{13}C$ of surface water particulate organic matter across the Subtropical Convergence in the SW Indian Ocean. Global Biogeochem. Cycles, 7: 627–644.

Gooday, A.J., 1986. Meiofaunal foraminiferans from the bathyal Porcupine Seabight (northeast Atlantic): size structure, standing stock, taxonomic composition, species diversity and vertical distribution in the sediment. Deep-Sea Res., 33: 1345–1373.

Gooday, A.J., 1988. A response by benthic Foraminifera to the deposition of phytodetritus in the deep-sea. Nature, 332: 70–73.

Gooday, A.J. and Lambshead, P.J.D., 1989. Influence of seasonally deposited phytodetritus on benthic foraminiferal populations in the bathyal northeast Atlantic: the species response. Mar. Ecol. Prog. Ser., 58: 53–67.

Gooday, A.J., Levin, L.A., Linke, P. and Heeger, T., 1992. The role of benthic foraminifera in deep-sea food webs and carbon cycling. In: G.T. Rowe and V. Pariente (Editors), Deep-Sea Food Chains and the Global Carbon Cycle. Kluwer, Dordrecht, pp. 63–91.

Gooday, A.J. and Turley, C.M., 1990. Responses by benthic organisms to inputs of organic material to the ocean floor: a review. Philos. Trans. R. Soc. London, A 331: 119–138.

Gordon, A.L., 1972. Introduction: physical oceanography of the Southeast Indian Ocean. In: D.E. Hayes (Editor), Antarctic Oceanology II. The Australian – New Zealand Sector. Am. Geophys. Union, Washington, USA, pp. 3–9.

Griggs, G.B., Carey, Jr., A.G. and Kulm, L.D., 1969. Deep-sea sedimentation and sediment–fauna interaction in Cascadia Channel and on Cascadia Abyssal Plain. Deep-Sea Res., 16: 157–170.

Hays, J.D., Lozano, J.A., Shackleton, N.J. and Irving, G., 1976. Reconstruction of the Atlantic and western Indian Ocean sectors of the 18,000 B.P. Antarctic Ocean. In: R.M. Cline and J.D. Hays (Editors), Investigation of Southern Ocean Paleoceanography and Paleoclimatology. Geol. Soc. Am. Mem., 145: 337–374.

Hemleben, C., Spindler, M. and Anderson, O.R., 1989. Modern Planktonic Foraminifera. Springer, New York, 363 pp.

Herguera, J.C. and Berger, W.H., 1991. Paleoproductivity from benthic foraminifera abundance: glacial to postglacial

change in the west-equitorial Pacific. Geology, 19: 1173–1176.

Highley, E., 1968. The International Indian Ocean Expedition: Australia's Contribution. CSIRO Division of Fisheries and Oceanography, 28 pp.

Howard, W.R. and Prell, W.L., 1992. Late Quaternary surface circulation of the Southern Indian Ocean and its relationship to orbital variations. Paleoceanography, 7: 79–117.

Howard, W.R. and Prell, W.L., 1994. Late Quaternary $CaCO_3$ production and preservation in the Southern Ocean: Implications for oceanic and atmospheric carbon cycling. Paleoceanography, 9:453–482.

Hutson, W.H., 1977. Variations in planktonic foraminiferal assemblages along north–south transects in the Indian Ocean. Mar. Micropaleontol., 2: 47–66.

Jacques, G. and Minas, M., 1981. Production primaire dans le secteur indien de l'océan Antarctique en fin d'été. Oceanol. Acta, 4: 33–41.

James, N.P., Bone, Y., von der Borch, C.C. and Gostin, V.A., 1992. Modern carbonate and terrigenous clastic sediments on a cool water, high energy, mid-latitude shelf: Lacepede, southern Australia. Sedimentology, 39: 877–903.

Jones, H.A. and Davies, P.J., 1983. Superficial Sediments of the Tasmanian Continental Shelf and Part of Bass Strait. Bur. Miner. Resour., Geol. Geophys. Bull., 218, 25 pp.

Kolla, V., Sullivan, L., Streeter, S.S. and Langseth, M.G., 1976. Spreading of Antarctic Bottom Water and its effects on the floor of the Indian Ocean inferred from bottom-water potential temperature, turbidity, and sea-floor photography. Mar. Geol., 21: 171–189.

Labracherie, M., Labeyrie, L.D., Duprat, J., Bard, E., Arnold, M., Pichon, J.-J. and Duplessy, J.-C., 1989. The last deglaciation in the Southern Ocean. Paleoceanography, 4: 629–638.

Le, J. and Shackleton, N.J., 1992. Carbonate dissolution fluctuations in the Western Equitorial Pacific during the Late Quaternary. Paleoceanography, 7: 21–42.

Lohmann, G.P., 1995. A model for variation in the chemistry of planktonic foraminifera due to secondary calcification and selective dissolution. Paleoceanography, 10: 445–457.

Loubere, P., 1991. Deep-sea benthic foraminiferal response to a surface ocean productivity gradient: a test. Paleoceanography, 6: 193–204.

Lutjeharms, J.R.E., Walters, N.M. and Allanson, B.R., 1985. Oceanic frontal systems and biological enhancement. In: W.R. Siegfried, P.R. Condy and R.M. Laws (Editors), Antarctic Nutrient Cycles and Food Webs. Springer, New York, pp. 11–21.

Lutze, G.F. and Coulbourn, W.T., 1984. Recent benthic foraminifera from the continental margin of Northwest Africa: community structure and distribution. Mar. Micropaleontol., 8: 361–401.

Mackensen, A., Sejrup, H.P. and Jansen, E., 1985. The distribution of living benthic foraminifera on the continental slope and rise off southwest Norway. Mar. Micropaleontol., 9:275–306.

Mackensen, A., Hubberten, H.-W., Bickert, T., Fischer, G. and Futterer, D.K., 1993. The $\delta^{13}C$ in benthic foraminiferal tests of *Fontbotia wuellerstorfi* (Schwager) relative to the $\delta^{13}C$ of dissolved inorganic carbon in Southern Ocean Deep Water: Implications for glacial circulation models. Paleoceanography, 8: 587–610.

Mallet, C.D. and Heezen, B.C., 1977. Circum-polar circulation and Late Tertiary changes in the Carbonate Compensation Depth south of Australia. Mar. Geol., 23: 89–101.

Martinez R., J.I., 1994a. Late Pleistocene carbonate dissolution patterns in the Tasman Sea. In: G. van der Lingen, K.M. Swanson and R.J. Muir (Editors), Evolution of the Tasman Sea Basin. Balkema, Rotterdam, pp. 215–228.

Martinez, J.I., 1994b. Late Pleistocene palaeoceanography of the Tasman Sea: Implications for the dynamics of the warm pool in the western Pacific. Palaeogeogr. Palaeoclimatol. Palaeoecol., 112: 19–62.

Martinson, D.G., Pisias, N.G., Hays, J.D., Imbrie, J., Moore Jr., T.C. and Shackleton, N.J., 1987. Age dating and the Orbital Theory of the Ice Ages: Development of a high-resolution 0 to 300,000-year chronostratigraphy. Quat. Res., 27: 1–29.

Matsuoka, H. and Okada, H., 1989. Quantitative analysis of Quaternary nannoplankton in the Subtropical Northwest Pacific Ocean. Mar. Micropaleontol., 14: 97–118.

McCartney, M.S., 1977. Subantarctic mode water. In: M. Angel (Editor), A Voyage of Discovery. Pergamon, Oxford, pp. 103–119.

Morley, J.J., 1989. Variations in high-latitude oceanographic fronts in the southern Indian Ocean: An estimation based on faunal changes. Paleoceanography, 4: 547–554.

Morley, J.J., Prell, W.L. and Howard, W.R., 1988. Response of the Southern Ocean over the Milankovitch frequency band. Eos, Trans. Am. Geophys. Union, 69: 299.

Nelson, C.S., Cooke, P.J., Hendy, C.H. and Cuthbertson, A.M., 1993. Oceanographic and climatic changes over the past 160,000 years at Deep Sea Drilling Project Site 594 off southeastern New Zealand, Southwest Pacific Ocean. Paleoceanography, 8: 435–458.

Osborne, N.I., Ciesielski, P.F. and Ledbetter, M.T., 1983. Disconformities and paleoceanography in the Southeast Indian Ocean during the past 5.4 million years. Geol. Soc. Am. Bull., 94: 1345–1348.

Park, Y.-H., Gamberoni, L. and Charriaud, E., 1993. Frontal structure, water masses and circulation in the Crozet Basin. J. Geophys. Res., 98: 12,361–12,385.

Parker, F.L., 1962. Planktonic foraminiferal species in Pacific sediments. Micropaleontology, 8: 219–254.

Passlow, V., 1994. Late Quaternary History of the Southern Ocean Offshore Southeastern Australia, Based on Deep-Sea Ostracoda. Ph.D. Thesis, Aust. Natl. Univ.

Passlow, V., Ayress, M.A. and Wells, P., in prep. Detection of downslope transport in deep-sea cores using shallow-water ostracods: evidence from the Southern Ocean.

Pichon, J.-J., Labeyrie, L.D., Bareille, G., Labracherie, M., Duprat, J. and Jouzel, J., 1992. Surface water temperature changes in the high latitude of the southern hemisphere over the last glacial–interglacial cycle. Paleoceanography, 7: 289–318.

Pisias, N.G., Martinson, D.G., Moore, T.C., Shackleton, N.J., Prell, W., Hays, J. and Boden, G., 1984. High resolution stratigraphic correlation of benthic oxygen isotopic records spanning the last 300,000 years. Mar. Geol., 56: 119–136.

Plancke, J., 1977. Phytoplankton biomass and productivity in the subtropical convergence area and shelves of the western Indian subantarctic islands. In: Proc. 3rd SCAR Symp. Antarctic Biology, Adaptations within Antarctic Ecosystems, pp. 51–37.

Prell, W.L., Hutson, W.H. and Williams, D.F., 1979. The Subtropical Convergence and Late Quaternary circulation in the Southern Indian Ocean. Mar. Micropaleontol., 4: 225–234.

Prell, W.L., Hutson, W.H., Williams, D.F., Bé, A.W.H., Geheitzenaur, K. and Molfino, B., 1980. Surface circulation of the Indian Ocean during the Last Glacial Maximum, approximately 18,000 yr B.P. Quat. Res., 14: 309–336.

Rathburn, A.E. and Corliss, B.H., 1994. The ecology of living (stained) deep-sea benthic foraminifera from the Sulu Sea. Paleoceanography, 9: 87–150.

Rathburn, A.E., Corliss, B.H., Tappa, K.D. and Lohmann, K.C., 1996. A comparison of living (stained) benthic foraminifera form the Sulu and South China Seas: observations on their ecology and stable isotopic compositions. Deep-Sea Res., 1996

Rochford, D.J., 1961. Hydrology of the Indian Ocean I. The water masses in intermediate depths of the South-East Indian Ocean. Aust. J. Mar. Freshwater Res., 12: 129–149.

Rochford, D.J., 1965. Rapid changes in the characteristics of the deep salinity maximum of the South-East Indian Ocean. Aust. J. Mar. Freshwater Res., 16: 129–149.

Rochford, D.J., 1977. A Review of a Possible Upwelling Situation off Port MacDonnell S.A. CSIRO Division of Fisheries and Oceanography Rep., 81, 4 pp.

Rodman, M.A. and Gordon, A.L., 1982. Southern Ocean Bottom Water of the Australian – New Zealand sector. J. Geophys. Res., 87: 5771–5778.

Saito, T., Thompson, P.R. and Breger, D., 1981. Systematic Index of Recent and Pleistocene Planktonic Foraminifera. Univ. Tokyo Press, 190 pp.

Schahinger, R.B., 1987. Structure of coastal upwelling events observed off the south-east coast of South Australia during February 1983 – April 1984. Aust. J. Mar. Freshwater Res., 38: 439–459.

Sen Gupta, B.K. and Machain-Castillo, M.L., 1993. Benthic foraminifera in oxygen-poor habitats. Mar. Micropaleontol., 20: 183–201.

Smart, C.W., King, S.C., Gooday, A.J., Murray, J.W. and Thomas, E., 1994. A benthic foraminiferal proxy of pulsed organic matter paleofluxes. Mar. Micropaleontol., 23: 89–99.

Tchernia, P., 1980. Descriptive Regional Oceanography. Pergamon, Oxford, 253 pp.

Thomas, E., Booth, L., Maslin, M. and Shackleton, N.J., 1995. Northeastern Atlantic benthic foraminifera during the last 45,000 years: changes in productivity seen from the bottom up. Paleoceanography, 10: 545–562.

van Harten, D., 1986. Use of ostracods to recognise downslope contamination in paleobathymetry and a preliminary reappraisal of the paleodepth of the Prasas Marls (Pliocene), Crete, Greece. Geology, 14: 856–859.

van Harten, D., 1990. Modern abyssal ostracod faunas of the eastern Mid-Atlantic Ridge area in the North Atlantic and a comparison with the Mediterranean. In: R. Whatley and C. Maybury (Editors), Ostracoda and Global Events. Chapman and Hall, London, pp. 321–328.

von der Borch, C.C. and Hughes-Clarke, J.E., 1993. Slope morphology adjacent to the cool-water carbonate shelf of South Australia: GLORIA and Seabeam imaging. Aust. J. Earth Sci., 40: 57–64.

Vincent, E. and Berger, W.H., 1981. Planktonic Foraminifera and their use in paleoceanography. In: C. Emiliani (Editor), The Oceanic Lithosphere. Wiley-Interscience, New York, pp. 1025–1119.

Wass, R.E., Conolly, J.R. and Macintyre, R.J., 1970. Bryozoan carbonate sand continuous along Southern Australia. Mar. Geol., 9: 63–73.

Williams, D.F., 1976. Late Quaternary fluctuations of the Polar Front and Subtropical Convergence in the Southeast Indian Ocean. Mar. Micropaleontol., 1: 363–375.